Hindawi
Shock and Vibration
Volume 2019, Article ID 5018732, 26 pages
https://doi.org/10.1155/2019/5018732

Research Article

Modal Parameters Identification Method Based on Symplectic Geometry Model Decomposition

Hang Jin, Jianhui Lin, Xieqi Chen, and Cai Yi

State Key Laboratory of Traction Power, Southwest Jiaotong University, Chengdu 610031, China

Correspondence should be addressed to Xieqi Chen; shayshe@msn.cn and Cai Yi; yicai@swjtu.edu.cn

Received 16 November 2018; Revised 13 May 2019; Accepted 15 July 2019; Published 11 September 2019

Guest Editor: Filipe Magalhaes

This paper proposes a novel method of structural system modal identification, where the iterative method is introduced in symplectic geometric model decomposition (SGMD). The proposed method can decompose the measured response into finite symplectic geometric components and identify the modal parameters of time-invariant structures and the instantaneous frequency of time-variant system through each symplectic geometric component. To obtain the shape information of the structural model, the SGCs of the same frequency at different measuring points are subjected to singular value decomposition (SVD). Both simulated data verification and measured data verification were used to verify if the method proposed in this article is effective for time-invariant system and time-variant system identification. For the simulated data, we study on a structural system which is set up with time-variant stiffness and time-invariant system. The measured vibration data of beam structure and time-variant wheel-rail coupling system were also tested and varied. Compared with the results of empirical model decomposition, the proposed method is capable of identifying instantaneous frequencies with better accuracy.

1. Introduction

The dynamic parameters are determined by the measured input and output of the vibration to establish a mathematical model for vibration systems. This method can be referred as the inverse problem of dynamics. Meanwhile, the experimental modal analysis was developed to solve this inverse problem. Also, structural damage can be identified and evaluated by its modal parameters. Hence, the accurate modal parameters identification of structure has great significance [1]. For integral structures, like gearboxes and equipped vehicles, it is difficult to apply artificial excitation during modal testing. Therefore, modal parameters would be identified by using the output signals directly under environmental excitation. Compared with the traditional modal test of input and output, the direct identification of modal parameters using output signals has the advantages of simple measurement, neighbour sensitivity, repetition frequencies, and much closer to the real dynamic characteristics [2].

Since structures are usually influenced by the environmental excitations, operational modal recognition methods, for example, the time-domain decomposition method [3], frequency domain decomposition method [4], and the stochastic subspace recognition method [5], were utilized in mechanical engineering structures by means of only output responses. For the problem of modal identification of structure which has a free vibration response, eigensystem realization algorithm (ERA) [6] was proposed. The applicability of the algorithm described above has been increased for using modal parameters identification under environmental excitation. Additionally, two methods, i.e., the random decrement method [7] and natural excitation method [8], were developed. It was shown that the random decrement function and correlation function have similar properties as the free decay vibration responses. This property can be employed in the identification of modal information. Dohler et al. [9] quantified the uncertainty effect in the modal identification by improving the traditional stochastic subspace identification method. Bayesian methods [10–13] were also proposed for identification of operational modals, which consider the noise effect as well as the uncertainty emerged in the real data. The above-mentioned methods were successfully employed to identify the vibration property for real structure [14–16].

However, it is known that the abovementioned methods mainly dealt with the problem of modal identification of time-invariant linear systems. When the tests are applied to the first structure prototype, nonlinearity is usually encountered [17]. Nonlinearity can obtain complicated dynamic phenomena, e.g., modal interactions, quasiperiodicity, and chaos subharmonic and superharmonic resonances, besides distorted resonances as well as the jumps between low- and high-amplitude responses. Therefore, essentially linear models are difficult in predicting the structural response [18]. For example, changes in the locations of the moving vehicle can lead to variations in the frequencies of a bridge-vehicle system [19]. Meanwhile, track irregularity would also be the cause of nonlinearity [20]. In this condition, proper understanding and identification of the vibration characteristics are significant. For example, time-variant frequency is essential to identify possible damage in the structure and to monitor the structural operational conditions.

The instantaneous frequency (IF) and instantaneous amplitude (IA) of system responses depend on damping and stiffness of the systems [21]. For this reason, Mihalec et al. [22] studied the synchrosqueezing wavelet transform (SWT) to apply free-response signal to recognize the damping ratio in the vibrating system.

It was shown that SWT with a proportional criterion gave relatively improved localization and estimation of damping ratios for close model, to minimize frequency-shift errors in original SWT. Montejo and Vidot-Vega [23] tested SWT by means of the estimated damping values of the structure from its noise-contaminated response, and it was concluded that SWT outperformance was greater than CWT and Hilbert–Huang transform when estimating the modal damping ratio. Li et al. [24] monitored the variations in structural responses by means of the EMD and wavelet analysis. Shi and Law [25] employed HHT to obtain the structural parameters in time-variant structure which have complete measurement responses. This technique is more accurate than traditional methods in identifying the damage occurrence and severity. Also, Ni et al. [26] employed variational model decomposition (VMD) to produce a few intrinsic model functions by decomposing the real responses and then utilized the Hilbert transform of each intrinsic model function to identify the instantaneous frequencies of time-variant systems. In the experiments, we analyze the real vibration data in the laboratory from a time-variant bridge-vehicle and a steel frame structure system. Unfortunately, the existing methods have at least one of the following defects:

(1) This method inevitably decomposes it to inaccurate components in the case of a complex (nonsinusoidal) waveform

(2) This method does not have noise robustness as it cannot effectively decompose signals with noises

(3) This method is very sensitive to the parameters, which are required to be defined by users

The analysis method proposed in this paper, which is based on symplectic geometry, has a protective effect on geometry structure of phase space, which represents system state variables. Also, the symplectic geometric decomposition method is primarily utilized to solve eigenvalue problem $2n \times 2n$. Hamiltonian matrix has been commonly used in dynamics and control systems, and rapidly employed to describe partial and singular differential equations, as well as other systems. In the method of symplectic geometric analysis, symplectic geometry spectrum analysis (SGSA) can preserve the essential characteristics of measurement and keep the main time series same as before; therefore, it is suitable for analyzing nonlinear systems [27, 28]. SGMD uses symplectic geometry spectrum analysis (SGSA) to solve the eigenvalues of the Hamiltonian matrixes and reconstructs individual symplectic geometric component signals (SGCs) with the corresponding eigenvectors. According to the authors' knowledge, there are no studies which use relatively new techniques to modal parameters identification. This paper applies the newly proposed SGMD technique to perform the signal decomposition of real responses from the structure systems and then their modal parameters identification.

This paper firstly introduced the theoretical analysis as well as the detailed algorithm process of symplectic geometric modal analysis. It is also proposed an improved iterative termination conditions for SGMD. We considered the modal responses on a structure, which is found in all sensor locations, to acquire the model shape corresponding to a particular model. The same frequency at different locations has been processed to singular value decomposition (SVD) in SGCs for obtaining modal models. Secondly, we analyzed the simulation study of structural response under impact force and verified the effectiveness of this method in identifying time-invariant modal parameters and time-variant instantaneous frequencies. Finally, the experimental research is implemented on beam structure and time-variant vehicle body vibration data. Compared with the existing technique, the proposed method is much better.

2. Theoretical Background

2.1. Motion Equation of Time-Variant Structure. The motion equation of a time-variant structure with n degrees of freedom (DOFs) is described by

$$M\ddot{x}(t) + C\dot{x}(t) + K(t)x(t) = BF(t), \tag{1}$$

where $K(t)$, C, and M mean stiffness matrices, damping, and $n \times n$ time-variant mass, respectively; $\ddot{x}(t)$, $\dot{x}(t)$, and $x(t)$ mean displacement response vectors, velocity, and acceleration of structure, respectively; and $F(t)$ is the applied excitation force on the structure with mapping matrix B and relates the applied excitation force to the corresponding DOFs. In this paper, the mass and damping matrices are time invariant, the variations of which are generally much smaller and insignificant compared to that of structural stiffness.

The frequency (variation) of each model will be narrow band if the coefficient has a minor time variation. According to the modal superposition method with n vibrational modal responses, we can obtain the structural displacement and

acceleration responses based on the principle of modal superposition. The signal is expressed with

$$x(t) = \sum_{i=1}^{n} \mathbf{\Phi}_i(t) q_i(t),$$
$$\ddot{x}(t) = \sum_{i=1}^{n} \mathbf{\Phi}_i(t) \ddot{q}(t), \tag{2}$$

where $\mathbf{\Phi}_i$ means i-th model shape and $q_i(t)$ is corresponding modal response. Based on the orthogonal property of model shape, equation (1) can be decoupled into equations of n models after substituting equation (2) in equation (1):

$$\ddot{q}_i(t) + 2\xi_i \omega_i(t) \dot{q}_i(t) + \omega_i^2 q_i(t) = \frac{\mathbf{\Phi}_i^T(t) F(t)}{m_i}, \tag{3}$$

where m_i, ξ_i, and ω_i are circular modal frequency, modal damping ratio, and the i-th modal mass, respectively. After an impulse force is employed to the z-th DOF, the the i-th generalized modal coordinate will have an acceleration response described as

$$\ddot{q}_i(t) = \frac{F_0 \phi_{zi,t=0} \omega_i(t)}{m_j \sqrt{1-\xi_i^2}} \exp\left(-\xi_i \omega_i(t)\right) \cos\left(\omega_{di}(t) t + v_i\right), \tag{4}$$

where $\phi_{zi,t=0}$ denotes the z-th item of the i-th modal vector $\mathbf{\Phi}_i(t)$ at time $t = 0$, $\omega_{di} = \omega_i \sqrt{1-\xi_i^2}$, and v_i is the phase angle.

The acceleration response $\ddot{x}_p(t)$ of the structure at the p-th DOF is as follows:

$$\ddot{x}_p(t) = \sum_{i=1}^{n} \phi_{pi}(t) \ddot{q}_i(t). \tag{5}$$

We can further write equation (5) as the superposition of amplitude-modulated-frequency-modulated signals:

$$\ddot{x}_p(t) = \sum_{i=1}^{n} S_i(t) = \sum_{i=1}^{n} A_i(t) \cos\left(\omega_{di}(t) t + v_i\right),$$
$$A_i(t) = \frac{\phi_{pi}(t) F_0 \phi_{zi,t=0} \omega_i(t)}{m_i \sqrt{1-\xi_i^2}} \exp\left(-\xi_i \omega_i(t)\right). \tag{6}$$

2.2. SGMD for Signal Decomposition. A trajectory matrix has been built by the SGMD method in the original time series during embedding. Firstly, the power spectral density (PSD) method is employed for obtaining the embedding dimension and the trajectory matrix. Then, the symplectic matrix is constructed, and the eigenvalues of Hamiltonian matrix are solved by symplectic geometric similarity transformation. Traditional SGMD obtains all SGC by similarity comparison. In this paper, SGC is extracted by merging all similar vectors of the maximum eigenvalue from the original signal and re-symplectic geometric model decomposition of residual components, which is an iterative process. To estimate the original time series in this study, we apply a diagonal averaging method to every symplectic principal component matrix. Figure 1 shows the diagram of SGMD technique.

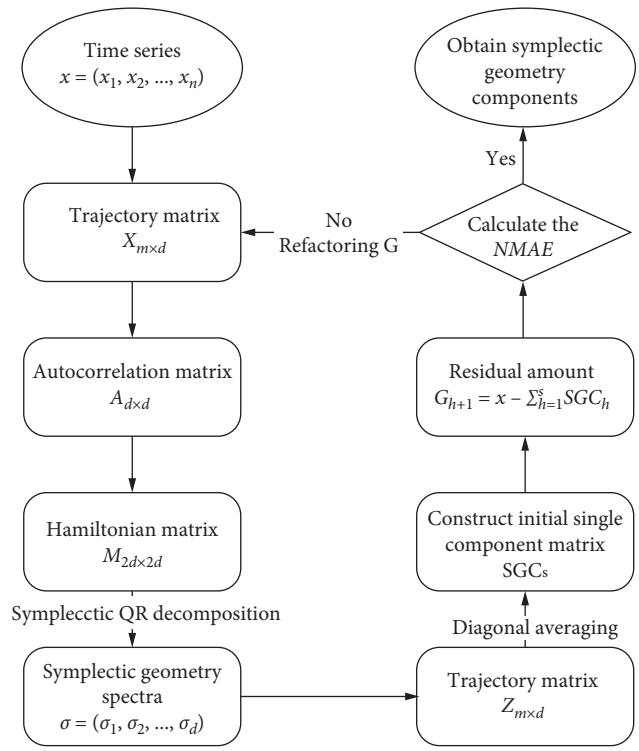

Figure 1: Block diagram of SGMD.

Before analyzing SGMD method, some definitions and theorems are introduced as follows.

Definition 1. S is a symplectic matrix if there is $\mathrm{JSJ}^{-1} = S^{-T}$.

Definition 2. H is a Hamiltonian matrix if there is $\mathrm{JHJ}^{-1} = -H^{-T}$.

Theorem 1. *For any symplectic matrix $A_{n\times n}$, construct a new matrix $M = \begin{bmatrix} A & 0 \\ 0 & -A^T \end{bmatrix}$; M is also a Hamilton matrix.*

Theorem 2. *Suppose the Householder matrix is supposed as*

$$H = H(k, w) = \begin{bmatrix} P & 0 \\ 0 & P \end{bmatrix},$$
$$P = I_n - \frac{2\overline{w}\,\overline{w}^{\mathrm{T}}}{\overline{w}^{\mathrm{T}}\overline{w}}, \tag{7}$$

where $\overline{w} = (0, \ldots, 0; w_k, \ldots, w_n)^T \neq 0$ and H is a symplectic unitary matrix.

Theorem 3. *Suppose an $m \times n (m > n)$ dimension real trajectory matrix X and $A = X^T X$ is a real symmetry matrix. Then, the Hamilton matrix M can be constructed from the symmetric matrix A, namely, $M = \begin{bmatrix} A & 0 \\ 0 & -A^T \end{bmatrix}$.*

There is a Householder matrix H; then, an upper Hessenberg matrix B is constructed via HMH^T, namely,

$$\begin{aligned} HMH^T &= \begin{pmatrix} P & 0 \\ 0 & P \end{pmatrix} \begin{pmatrix} A & 0 \\ 0 & -A^T \end{pmatrix} \begin{pmatrix} P & 0 \\ 0 & P \end{pmatrix}^T \\ &= \begin{pmatrix} PAP^T & 0 \\ 0 & -PA^TP^T \end{pmatrix} \\ &= \begin{pmatrix} B & 0 \\ 0 & -B^T \end{pmatrix}, \\ \lambda(A) &= \lambda(B), \\ \sigma &= \lambda^2(X) = \lambda(A). \end{aligned} \tag{8}$$

The upper Hessenberg matrix B is an n-dimension space matrix. Therefore, the primary $2n$-dimension space Hamilton matrix M can be resolved via transforming it into n-dimension space.

The key of symplectic geometry model decomposition is to utilize symplectic geometry spectrum analysis (SGSA) for solving the eigenvalues of Hamiltonian matrix and reconstructing the single component signals via its corresponding eigenvectors. Therefore, the power spectral density (PSD) method is applied to adaptively obtain embedding dimension of the studied time series. Then, symplectic geometry is constructed, and SGSA is used to deal with the eigenvalues of Hamiltonian matrix. Finally, the diagonal averaging and adaptive reconstruction are employed to obtain symplectic geometry components. Therefore, the SGMD may fit for nonlinear signal analysis.

The symplectic geometry model decomposition method usually can be divided into four parts: adaptive determining embedding dimension of the time series, solving the eigenvalues of Hamiltonian matrix via symplectic geometry similarity transformation, diagonal averaging, and adaptive reconstruction of components.

Briefly, any original signal time series are expressed as $x = x_1, x_2, \ldots, x_n$, ($n$ means data length). Based on Takens' theorem, a time-series delay topology equivalent method is used to reconstruct the multidimensional signals via one dimensional signal. That is to say the original time series can be projected to the trajectory matrix X which has all the dynamic information of time series x:

$$X = \begin{bmatrix} x_1 & x_{1+\tau} & \cdots & x_{1+(d-1)\tau} \\ x_2 & x_{2+\tau} & \cdots & x_{2+(d-1)\tau} \\ \vdots & \vdots & \vdots & \vdots \\ x_m & x_{m+\tau} & \cdots & x_{m+(d-1)\tau} \end{bmatrix}, \tag{9}$$

where d is the embedding dimension, τ is the delay time, $m = n - (d-1)\tau$, and the appropriate embedding dimension d and the delay time τ are chosen to get the corresponding reconstruction matrix. The idea of determining embedding dimension in the existing studies [29] is employed to calculate the PSD of the initial time series x. Subsequently, $f_{\max}$, frequency of the maximum peak, is estimated from PSD. d is set to $n/3$ where n is the length of data if the normalized frequency is less than the given threshold 10^{-3}. Otherwise, it is set to $d = 1.2 \times (Fs/f_{\max})$.

To obtain Hamiltonian matrix, autocorrelation analysis is implemented on the trajectory matrix to get the covariance symmetric matrix A:

$$A = X^T X. \tag{10}$$

Then, the Hamilton matrix M will be obtained based on the symmetric matrix A:

$$M = \begin{bmatrix} A & 0 \\ 0 & -A^T \end{bmatrix}. \tag{11}$$

After constructing Hamilton matrix, the square of M is N, i.e., $N = M^2$, and the matrices M and N are Hamilton matrices by the definition of Hamilton matrix. Therefore, a symplectic orthogonal matrix Q can be obtained from the following equation:

$$Q^T N Q = \begin{bmatrix} B & R \\ 0 & B^T \end{bmatrix}, \tag{12}$$

where Q means an orthogonal symplectic matrix with the property of its prototype, to protect the structure of Hamilton matrix when it is transformed. Here, B means upper triangular matrix, i.e., $b_{ij} = 0\,(i > j+1)$. It can be transformed via utilizing the Schmidt orthogonalization to matrix N, and the eigenvalue of the upper triangular matrix B can be calculated as $\lambda_1, \lambda_2, \ldots, \lambda_d$. Indeed, the eigenvalues of A will equal those of B if A is real symmetric. Based on the properties of Hamilton matrix, the eigenvalues of the matrix A are obtained:

$$\sigma_i = \sqrt{\lambda_i}, \quad i = 1, 2, \ldots, d. \tag{13}$$

The symplectic geometry of X is made by eigenvalues of A in descending order, i.e.,

$$\sigma_1 > \sigma_2 > \cdots > \sigma_d. \tag{14}$$

The distribution of σ_i is the symplectic geometry spectra of A, with its smaller values to be usually treated as noise components. $Q_i\,(i = 1, 2, \ldots, d)$ means eigenvectors which correspond to eigenvalue of matrix A.

Matrix Q is constructed as Householder matrix H from equation (14), where the theory of symplectic geometry can be employed to solve the embedding dimension time series. Therefore, the Householder matrix H, rather than the symplectic orthogonal matrix Q, has been selected. H is easy to be verified as the unitary matrix, and H can be obtained from real matrix. This is helpful for researching the time series. Moreover, let $S = Q^T X$, $Z = QS$, and Z be the reconstructed trajectory matrix. Each component matrix is reconstructed as per the following steps.

Firstly, based on the unitary matrix eigenvectors and trajectory matrix, the transformation coefficient matrix S is obtained as follows:

$$S_i = Q_i^T X^T. \tag{15}$$

Then, to obtain reconstruction matrix Z, the transformation coefficient matrix is transformed:

$$Z_i = Q_i S_i, \tag{16}$$

where Z_i $(i = 1, 2, \ldots, d)$ is the initial single component. Similarly, trajectory matrix Z is

$$Z = Z_1 + Z_2 + \cdots + Z_d. \tag{17}$$

The obtained initial single component matrix Z is $m \times d$ matrix. Therefore, the initial single component should be reordered, and the reconstructed matrix Z should be transformed by the diagonal averaging into a new set of time series of length n. Meanwhile, that of new time series d can be achieved as well, where the sum of new time series d is the original time series.

Additionally, we define the elements of matrix as z_{ij} for any initial single component matrix Z_i, where $1 \le i \le d$, $1 \le j \le m$, and $d^* = \min(m, d)$, $m^* = \max(m, d)$, and $n = m + (d-1)\tau$. Let $z^*_{ij} = z_{ij}$ if $m < d$; otherwise, $z^*_{ij} = z_{ji}$. Thus, the diagonal averaging transfer matrix is

$$y_k = \begin{cases} \dfrac{1}{k} \displaystyle\sum_{k}^{p=1} z^*_{p,k-p+1}, & 1 \le k < d^*, \\[2ex] \dfrac{1}{d^*} \displaystyle\sum_{d^*}^{p=1} z^*_{p,k-p+1}, & d^* \le k \le m^*, \\[2ex] \dfrac{1}{n-k+1} \displaystyle\sum_{n-m^*+1}^{p=k-m^*+1} z^*_{p,k-p+1}, & m^* < k \le n. \end{cases} \tag{18}$$

The matrix Z_i is transformed to a series of $Y_i(y_1, y_2, \ldots, y_n)$ based on equation (20). Thus, by diagonal averaging, we can transform the reconstruction matrix Z into a new series of matrix Y with the length $d \times n$. Additionally, it can decompose the original time series into d independent superimposed components with various trends and frequency bands.

d single component signals are acquired via diagonal averaging:

$$Y = Y_1 + Y_2 + \cdots + Y_d. \tag{19}$$

After construction of the trajectory matrix and implementation of diagonal averaging, d single components are obtained, whereas the components are not totally independent as they may have same characteristics, periods, and frequency components, which means that the initial single components with same characteristics need reconstructing. The component correlation and frequency similarity are employed to rebuild the components. Also, the components divided from a component will be rebuilt via calculating their frequency and correlation. Additionally, the signal usually includes numerous noise components irregularly, such as frequency and correlation as the interference of environmental factors. Therefore, it is urgent to set the iterative stopping conditions.

Firstly, the correlation was calculated with Y_1 and other reconstructed signals $Y_{k \ne l}$, and the highly similar Yk is composed of the first SGC component. Then the SGC_l is removed from the source signal x, and the residual signal is recorded as g_{h+1}:

$$g_{h+1} = x - \sum_{l=1}^{h} \mathrm{SGC}_l, \tag{20}$$

where h means number of iterations. Finally, the calculation would be made for normalized mean absolute error (NMAE) of the participating signals:

$$\mathrm{NMAE}_h = \frac{1}{t} \sum_{t=1}^{n} \left| \frac{g_{h+1}(t)}{x(t)} \right|. \tag{21}$$

The whole decomposition process will continue until the normalized mean absolute error is smaller than the predetermined threshold $\mathrm{NMAE}_h = 1\%$. Otherwise, the reconstructed residual signal g_h is the trajectory matrix X and the above $\mathrm{NMAE}_h = 1\%$ iterative process is repeated until the iteration termination condition is satisfied. And, the final decomposition result is obtained as follows:

$$x(t) = \sum_{h=1}^{N} \mathrm{SGC}_h(t) + g_{N+1}(t), \tag{22}$$

where N means number of identified component series. Different from the traditional SGMD method, the newly proposed SGMD removes the reconstructed signal Y_1 with the largest feature and its similar signal from the source signal. It also needs to take the judgement which reiled on the NMAE of residual signal for completing the decomposion, still, the method by continuing to search for the new SGC is replaced as the new trajectory matrix recalucation. This can be more accuary compared with combing the reconstructed signal Y in the conventional SGMD method for obtaining SGC. Hence, the iterative process has been added to improve the traditional SGMD.

2.3. Hilbert Transform. It is widely accepted that time-frequency analysis methods have advantages over the traditional methods. By using fast Fourier transformation (FFT), energy distribution in the time and frequency scales can be visualized with an adjustable resolution. Additionally, the signal in the frequency scale can be investigated with multiresolution analysis from time-frequency analysis via the time scale information. In areas of damage identification, modal identification, and signal processing, the time-frequency analysis methods are widely utilized. Performing the signal decomposition with SGMD, several SGCs are obtained and employed for obtaining Hilbert spectrum. Both nonlinear and nonstationary signals can be analyzed by Hilbert transform. To perform Hilbert transform using the extracted the SGCs from a vibration response signal, it is required to obtain frequency and time-domain information with the instantaneous frequencies and amplitudes. The following equation can be used to define Hilbert transform of a specific SGC:

$$\widetilde{\mathrm{SGC}}_k(t) = H\left[\mathrm{SGC}_k(t)\right] = \frac{1}{\pi} P \int_{-\infty}^{+\infty} \frac{\mathrm{SGC}_k(\tau)}{t-\tau} d\tau, \tag{23}$$

where $\widetilde{\mathrm{SGC}}_k(t)$ is the Hilbert transform of symplectic geometry components $\mathrm{SGC}_k(t)$ and P is the Cauchy principle value. The analytical signal is

$$z_k(t) = \mathrm{SGC}_k(t) + \widetilde{\mathrm{SGC}}_k(t) = A_k(t)e^{j\theta_k(t)},$$
$$A(t) = \left[\mathrm{SGC}_k(t)^2 + \widetilde{\mathrm{SGC}}_k(t)^2\right]^{1/2}, \tag{24}$$
$$\theta_k(t) = \arctan\left(\frac{\widetilde{\mathrm{SGC}}_k(t)}{\mathrm{SGC}_k(t)}\right).$$

Finally, the identified instantaneous frequency $\omega_{id}^k(t)$ of k-th component is expressed by

$$\omega_{id}^k(t) = \frac{\partial\theta_k(t)}{\partial t}. \tag{25}$$

2.4. Modal Data Identification Algorithm. Figure 2 shows the diagram for identifying modal characteristics by means of SGMD method for system identification. The diagram contains the following five main steps:

(1) The SGMD has been processed on n point sensor data $(x_1, x_2 \ldots, x_n)$ for test structure, each measurement point retains k SGC scale components, and data length is N:

$$\mathrm{SGC}_n = \begin{bmatrix} \mathrm{SGC}_n(a_1,t_1) & \mathrm{SGC}_n(a_1,t_2) & \cdots & \mathrm{SGC}_n(a_1,t_N) \\ \mathrm{SGC}_n(a_2,t_1) & \mathrm{SGC}_n(a_2,t_2) & \cdots & \mathrm{SGC}_n(a_2,t_N) \\ \vdots & \vdots & \vdots & \vdots \\ \mathrm{SGC}_n(a_k,t_1) & \mathrm{SGC}_n(a_k,t_2) & \cdots & \mathrm{SGC}_n(a_k,t_N) \end{bmatrix}_{k\times N}. \tag{26}$$

(2) Since the symplectic geometric decomposition will disturb the order of scales, it is necessary to compare the correlation coefficients of the SGC components of all sensors and select one SGC component with the largest correlation coefficient from different measuring points n to form N new matrices A_k:

$$A_k = \begin{bmatrix} W_1(a_k,t_1) & W_1(a_k,t_2) & \cdots & W_1(a_k,t_N) \\ W_2(a_k,t_1) & W_2(a_k,t_2) & \cdots & W_2(a_k,t_N) \\ \vdots & \vdots & \vdots & \vdots \\ W_n(a_k,t_1) & W_n(a_k,t_2) & \cdots & W_n(a_k,t_N) \end{bmatrix}_{n\times N}. \tag{27}$$

Thus, A_k can form a singular value decomposition matrix which can ensure to contain the same instantaneous frequency.

(3) Singular value decomposition for each combined matrix is carried out:

$$A_k = U_k S_k V_k^T, \tag{28}$$

where $U_k = \{u_{1k}, u_{2k}, \ldots, u_{nk}\}$; $S_k = (\sum_{\lambda k} O)$, $\sum_{\lambda k} = \mathrm{diag}(\sigma_{1k}, \sigma_{2k}, \ldots, \sigma_{nk})$; $V_k = \{v_{1k}, v_{2k}, \ldots, v_{nk}\}$.

(4) The judgement matrix is reconstructed by using the first singular value σ_{1k}:

$$B[\sigma_{11}, \sigma_{12}, \ldots, \sigma_{1k}]_{1\times k}. \tag{29}$$

In this formula, B represents the obtained first singular value of different scales decomposition.

(5) The first singular value vectors u_{1k} and v_{1k} are reconstructed to obtain the reconstructed matrix:

$$D_1 = [u_{11}, u_{12}, \ldots, v_{1k}]_{n\times k},$$
$$D_2 = [v_{11}, v_{12}, \ldots, v_{1k}]_{k\times N}. \tag{30}$$

When the scale point position of local maximum in B corresponds to a_l, D_1 contains structural point vibration model information and D_2 contains the natural frequency of structural modal point and its damping ratio:

$$\{\Phi_i\} = D_{1l},$$
$$\begin{cases} \omega_i = \sqrt{\left(\dfrac{d}{dt}\angle D_{2l}\right)^2 + \left(\dfrac{d}{dt}\left(\ln|D_{2l}|\right)\right)^2}, \\ \xi_i = \dfrac{-(d/dt)\left(\ln|D_{2l}|\right)}{\omega_i}. \end{cases} \tag{31}$$

l is the scale corresponding to the column a_l. $D_{1l} = u_{1l}$, $D_{2l} = v_{1l}$, and $\angle$ represents the phase angle.

3. Simulation Studies

Simulation studies are performed on a time-variant multi-DOF shear-type structure to explore the effectiveness of the proposed method for time-variant system identification. To verify the proposed method, a simulation model of 5-DOF mass-spring-damper is fabricated first, which is shown in Figure 3.

Also, based on equation (1) and the mass matrix M,

$$M = \begin{bmatrix} 4.9895 & 0 & 0 & 0 & 0 \\ 0 & 4.9895 & 0 & 0 & 0 \\ 0 & 0 & 4.9895 & 0 & 0 \\ 0 & 0 & 0 & 4.9895 & 0 \\ 0 & 0 & 0 & 0 & 4.9895 \end{bmatrix}, \tag{32}$$

and the stiffness matrix K of the model is

$$K = \begin{bmatrix} k_1 + k_{12} & -k_{12} & & & \\ -k_{12} & k_{12} + k_{23} & -k_{23} & & \\ & -k_{23} & k_{23} + k_{34} & -k_{34} & \\ & & -k_{34} & k_{34} + k_{45} & -k_{45} \\ & & & -k_{45} & k_5 + k_{45} \end{bmatrix}, \tag{33}$$

where $k_{12} = 17{,}110$ N/s, $k_{23} = 8005$ N/s, $k_{45} = 5632$ N/s, $k_5 = 13{,}300$ N/s, and k_1 and k_{34} are the time-variant stiffness parameters. Three cases with periodical and smooth variations are researched, respectively. The variant stiffnesses in Case 1 are set as $k_1 = 2000$ N/m and $k_{34} = 48{,}000$ N/m, which is a time-invariant system, and defined as $k_1 = (5 - 0.08t) \times 10^3$ N/s and $k_{34} = (4.8 - 0.12 * t) \times 10^4$ N/s in Case 2. The corresponding values in Case 3 are $k_1 = (2 + 0.6\sin(2\pi t)) \times 10^3$ N/m and $k_{34} = 48{,}000$ N/m.

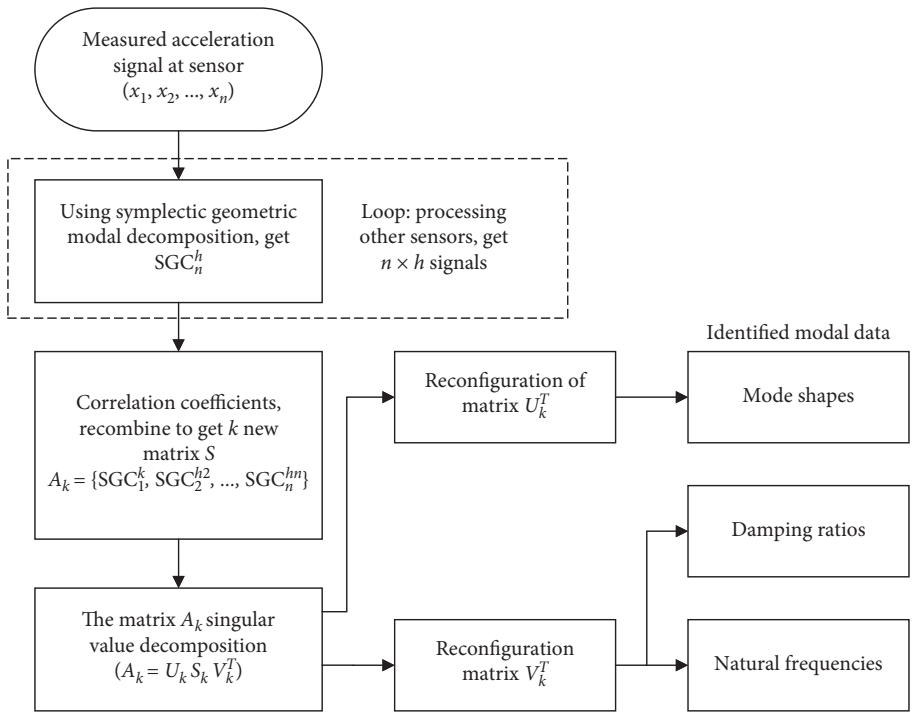

Figure 2: Workflow of the proposed modal data identification method.

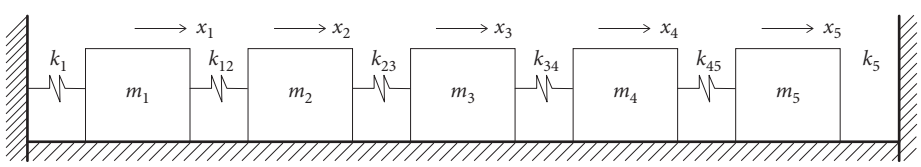

Figure 3: The 5-DOF simulation model.

Proportional damping $C = 0.08M$. The following impulse force is applied at the fourth layer:

$$BF(t) = \begin{Bmatrix} 0 \\ 0 \\ 0 \\ f(t) \\ 0 \end{Bmatrix}, \quad f(t) = \begin{cases} 500\,\text{N}, & t = 0, \\ 0, & t \neq 0. \end{cases} \tag{34}$$

Newmark beta method, a time-stepped integration method, is used to solve the analytical responses of time-variant system. 200 Hz is set as the sampling frequency. The acceleration signal from the top level is chosen to decompose signals and identify the following instantaneous frequencies. Moreover, the signal-to-noise ratio of vibration signals in both three cases is 30 dB, which is considered the noise effect in measurement.

3.1. Linear Structure Modal Identification. According to the structural parameters of Case 1, the modal shape can be obtained as

$$\Phi = \begin{bmatrix} 1.0000 & 1.5690 & -0.4609 & 4.4280 & 0.3353 \\ 1.0352 & 1.0000 & 0.0231 & -5.3460 & -1.6530 \\ 0.9295 & -1.2411 & 1.0000 & 0.3206 & 15.4604 \\ 0.8848 & -1.4027 & 0.7469 & 1.0000 & -15.0077 \\ 0.2842 & -0.7365 & -4.0584 & -0.2703 & 1.0000 \end{bmatrix}. \tag{35}$$

The natural frequencies can be obtained as $f_1 = 2.66438$ Hz, $f_2 = 6.4540$ Hz, $f_3 = 10.0685$ Hz, $f_4 = 14.2087$ Hz, and $f_5 = 22.9175$ Hz. The damping ratios for each order are obtained as $\xi_1 = 0.1066$, $\xi_2 = 0.2582$, $\xi_3 = 0.4027$, $\xi_4 = 0.5683$, and $\xi_5 = 0.9167$. Still, the modal assurance criterion (MAC) is utilized for the evaluation of the errors of identified model shape:

$$\text{MAC}_i = \frac{\left(\phi_i^T \widehat{\phi}_i\right)^2}{\phi_i^T \phi_i \widehat{\phi}_i^T \widehat{\phi}_i}, \tag{36}$$

where ϕ_i is the estimated model vector and $\widehat{\phi}_i$ is the theoretical one. Figure 4 shows the Fourier transform spectrum and time history of the response signal from Case 1. The Fourier spectrum clearly indicates five frequencies.

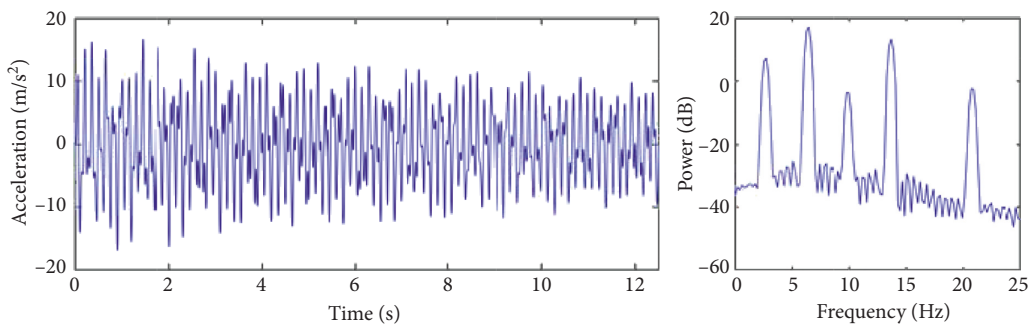

Figure 4: Time-domain response signals as well as the fast Fourier transform spectrum in the simulation study (Case 1).

Unlike the SGMD method introduced in reference [28], in order to suppress overdecomposition, equation (23) described in this paper is used as the iteration termination condition, and the simulation signal is decomposed into five SGCs. The symplectic geometric decomposition of the vibration signal on the fifth degree of freedom is shown in Figure 5. After the decomposition, the order of each layer for SGC is not arranged in the sequence of frequency but followed the energy distribution; the order of sequences has been rearranged in order to natural frequency identification. The SGMD can decompose each order of vibration into independent components. Meanwhile, modal shapes cannot be obtained after decomposing a single signal. This paper proposes to combine SGMD with SVD and identify the modal parameters of the reconstructed matrix D_2 as shown in Figure 6. Also, each individual component is close to the vibration of a single degree of freedom. At the same time, according to D_1, the model shape can be obtained.

The modal parameters of linear simulation signal are identified by the methods of SVD, SGMD, and SGMD-SVD, respectively. The results are shown in Table 1. The SVD can effectively identify the model shape, but the natural frequency and damping ratio recognition effect are very unsatisfactory. After SGMD classifies a single simulation signal, the identified natural frequency and damping are more accurate and the fifth-order natural frequency identification result has a larger deviation, owing to fact that the simulation signal has a shorter step size and the affected recognition frequency is lower. The combination of SGMD and the SVM, not only effectively identify models but also can be effective for identifying the natural frequency and damping for simulation modal identification signals. Therefore, the SGMD can decompose the measured signals into each effective frequency single signal, which is convenient for the identification of modal parameters. Still, the vibration models were extracted by SVD, and MAC values were all greater than 0.898. As a result, the proposed method is suitable and applicable to the identification of linear modal parameters.

3.2. Nonlinear Structure Instantaneous Frequency Identification. Figure 7 shows the Fourier transform spectrum and the time history of the response signal in Case 2. The Fourier spectrum has five frequencies, as shown in Figure 7. Thus, signal decomposition is implemented via SGMD. The decomposed SGCs as well as their corresponding frequency spectra are shown in Figure 8. Four independent frequency components are decomposed in the Fourier spectra, which are well separated. The true and identified instantaneous frequencies of time-variant structure are shown in Figure 9. Note that the "freezing method" is used to obtain the theoretical instantaneous frequency [30]. Assume that, in each time interval, the structural physical parameters are unchanged, and the theoretical instantaneous frequency is solved from the solution of eigenvalue analysis problem. The finite duration of measured signals will have an end effect, which may bring certain errors, especially when the response signals begin and stop, which is shown in Figure 9. In general, with the associated FFT analysis, the end and leakage effects are significant. In addition, employing FFT with band-pass filters cannot identify the instantaneous frequency of time-variant systems. Meanwhile, the proposed approach can successfully identify the smooth decreasing time-variant frequencies.

From the Fourier transform of SGCs in Figure 8(c), the decomposed signals still have a modal aliasing problem. Observing the time-domain map is not difficult to find, which is caused by modal aliasing caused by the endpoint effect.

Figures 10–12 show the identified instantaneous frequencies, decomposed SGC via SGMD, and the response signal in time and frequency domains for Case 3, respectively. As shown in Figure 11, the Fourier spectra of the decomposed SGCs indicate that the five models are clearly decomposed. Similar to Figure 8(c), the end effect mode results still lead to the certain aliasing in Figure 11(c) and 11(d).

Moreover, Figure 12 shows the identified instantaneous frequencies where the lower frequency component has larger variation compared to its higher counterpart. Nevertheless, the identified first models are the best among all the models. The high model offsets the central frequencies caused by noise, while the identified low model frequency fluctuates around the central frequency.

Empirical model decomposition (EMD), a typical method for signal decomposition, is also employed in this study for the vibration response of Case 3 (Figure 13 shows the obtained IMFs). The results of the first two decomposition in EMD are similar to those in the proposed method in this paper. The instantaneous frequency of IMF1

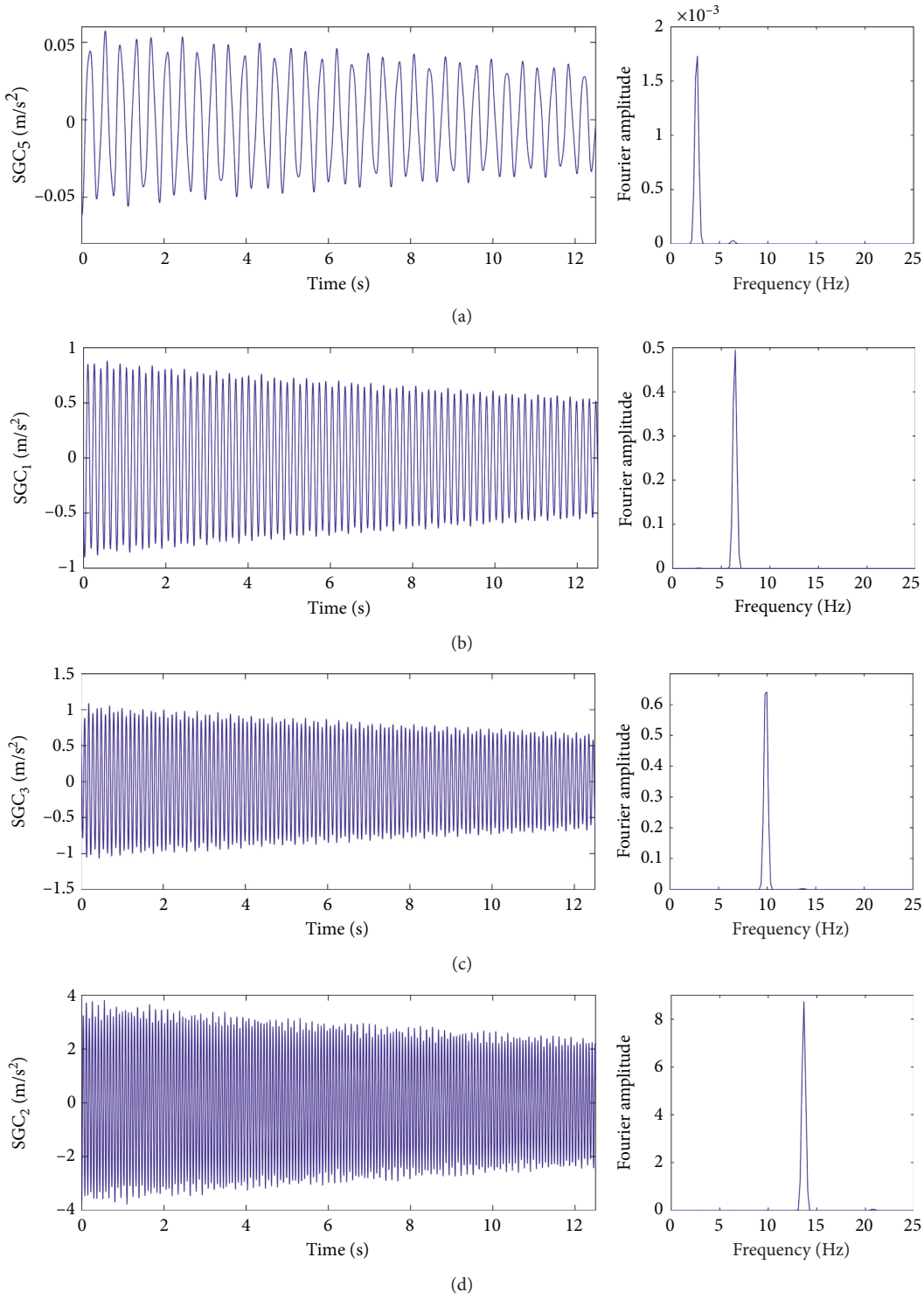

Figure 5: Continued.

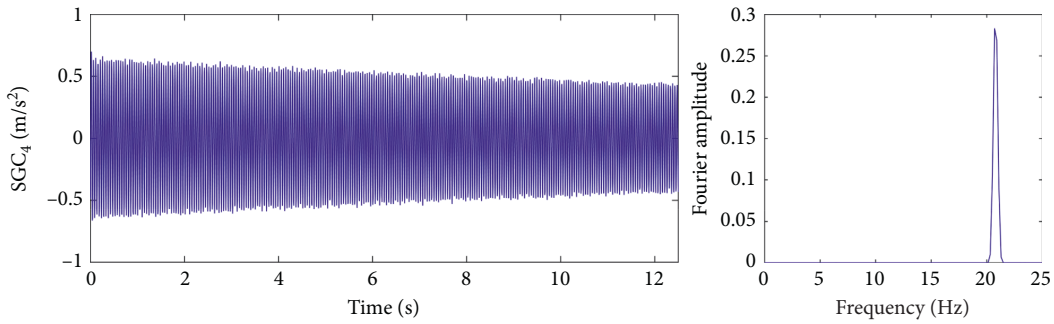

(e)

Figure 5: The results of the symplectic geometry decomposition and power spectrum for DOF5.

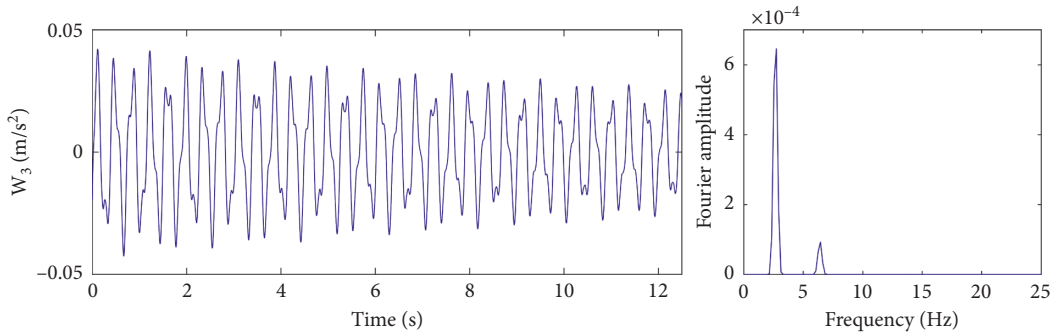

(a)

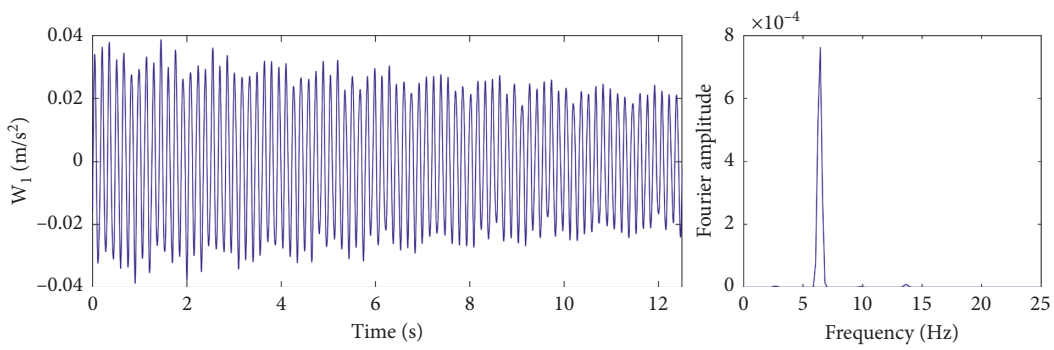

(b)

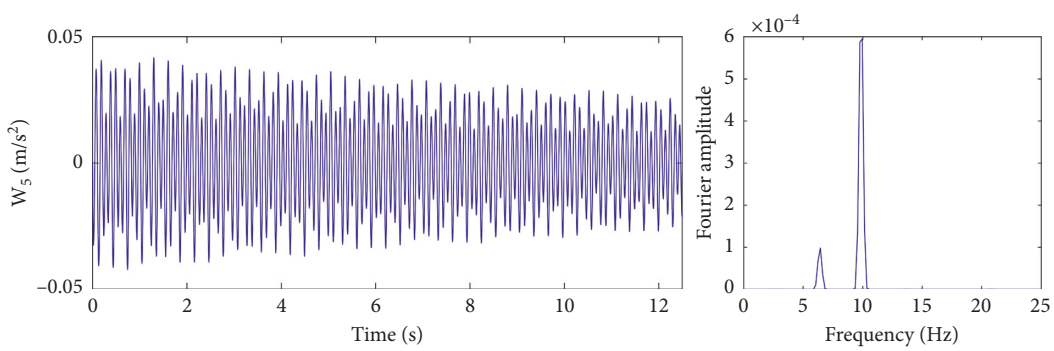

(c)

Figure 6: Continued.

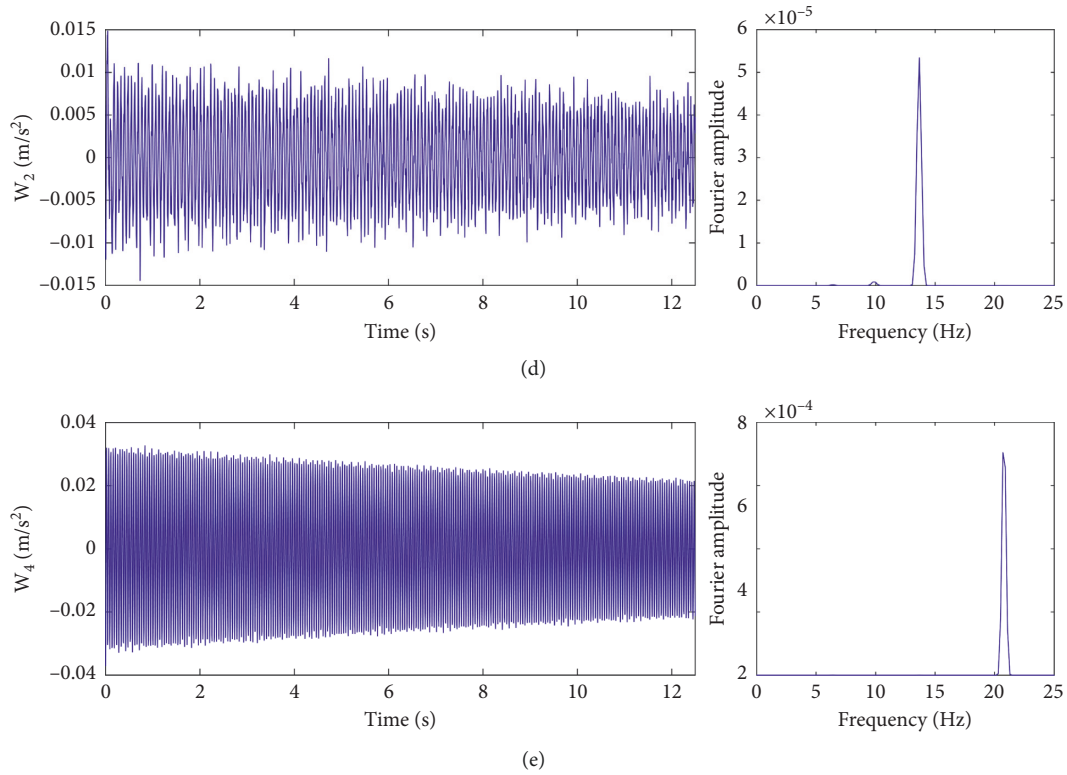

Figure 6: The matrix reconstruction for D_2 in SGMD-SVD.

and IMF2 has been overlapped, which is approximated as the component of theoretical instantaneous frequency 5. In the results of EMD decomposition, there is no component that coincides with the theoretical instantaneous frequencies 3 and 4. Therefore, it is difficult to decompose signals from time-variant systems. Figure 10 demonstrates that the Fourier spectrum has several peaks within a scope of the most significant frequency components, which means that it is relatively difficult for the traditional methods to realize the signal decomposition. As shown in Figures 13 and 14, significant fluctuations are observed as the noise in measurements influences the performance of EMD in signal decomposition.

As shown in Figures 12 and 14, comparing the results of SGMD and EMD, SGMD has much better performance for instantaneous frequency identification and the signal decomposition.

3.3. Effect of Measurement Noise. Noise was added to the response simulation of Case 3 to carry out the further study on robustness of method for modal identification using SGMD, and the signal-to-noise ratio was 10 dB and 20 dB, respectively. To decrease the high frequency noise, the noisy responses are processed by a band-pass filter with a frequency range of 1 ~ 30 Hz due to the fact that the first five are observed within 30 Hz. For SGMD employed for signal decomposition, the same procedure is followed, and the obtained instantaneous frequencies are recognized and shown in Figure 15. As shown in Figure 15, all the five frequency models are in a complete separation state and the true values are close with the identified instantaneous frequencies. As a result, the results on the first model show the best agreement. Therefore, it can be seen from the above that the first model dominates the vibration. Moreover, the results of models 2 and 5 under such high noise effects are also satisfactory.

It can be seen that the SGMD method is applicable to both modal parameter identification of linear systems and instantaneous frequency of nonlinear systems. Compared with the traditional EMD and SVD identification methods, SGMD has better robustness and adaptability.

4. Experimental Verifications

SGMD can be used to decompose linear and nonlinear signals. The existing methods, due to end effects or time-variant systems with nonstationary signals, still have some limitations when it comes to processing signals from time-invariant systems. In order to explore the performance of instantaneous frequency identification in the mechanical structure using the proposed method in this case, experimental studies on both time-variant and time-invariant systems were performed in the laboratory. The proposed method is used to extract the instantaneous frequency of the structure, and the real vibration data are used for signal decomposition. An experimental study of the first invariant structure was employed to prove the accuracy of proposed method, with particular attention on how to use the

Table 1: Comparison of modal parameter identification results.

Model	SVD					SGMD				SGMD-SVD				
	Natural frequency	Error (%)	Damping ratio	Error (%)	MAC	Natural frequency	Error	Damping ratio	Error (%)	Natural frequency	Error (%)	Damping ratio	Error (%)	MAC
1	2.204774	17.25	0.128879	20.90	0.904	2.660464	0.15%	0.105204	1.31	2.660789	0.13	0.10789	1.21	0.959
2	6.433347	0.32	0.267495	3.60	0.77	6.39942	0.85%	0.255257	1.14	6.399353	0.85	0.254756	1.33	0.898
3	9.653678	4.12	0.488475	21.30	0.973	9.864816	2.04%	0.396764	1.47	9.864922	2.04	0.407428	1.17	0.952
4	24.27983	70.88	0.20743	63.50	0.964	13.65411	3.98%	0.558576	1.71	13.67084	3.86	0.553462	2.61	0.914
5	56.19371	145.20	0.035751	96.10	0.958	20.79091	9.73%	0.796246	13.14	20.79083	9.73	0.777912	15.14	0.948

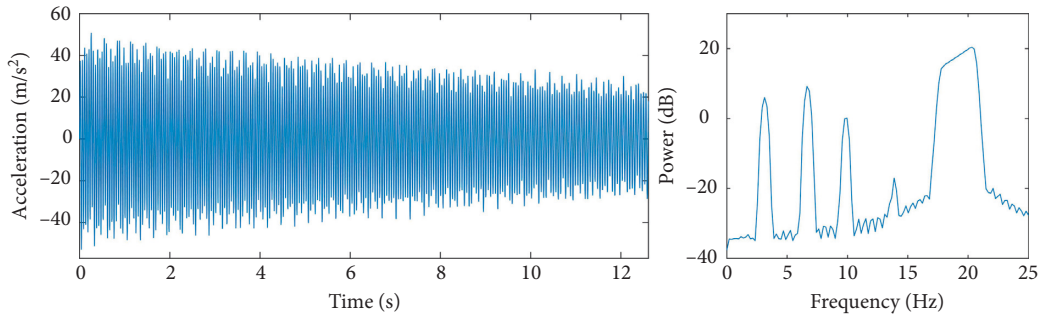

Figure 7: Time-domain response signal and its fast Fourier transform spectrum in the simulation study (Case 2).

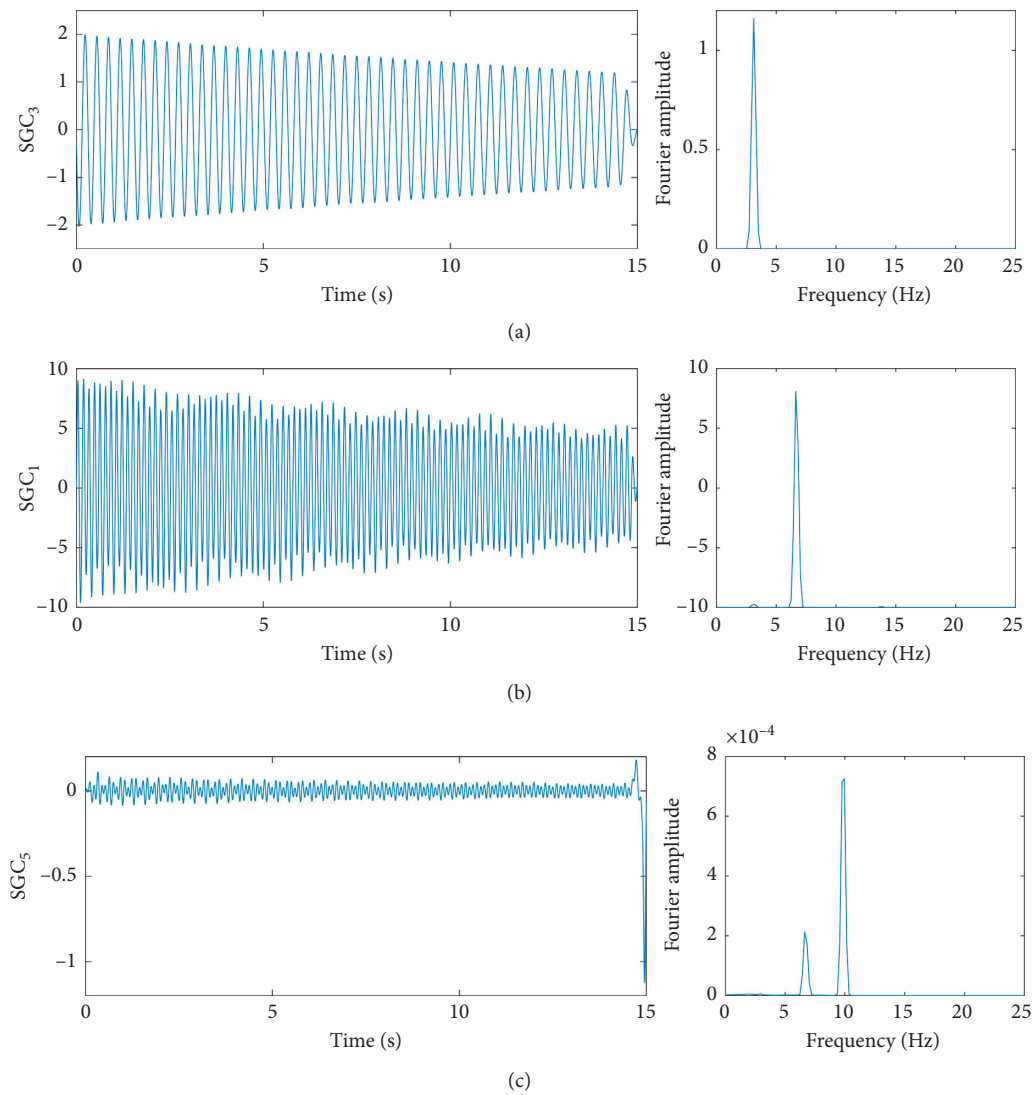

Figure 8: Continued.

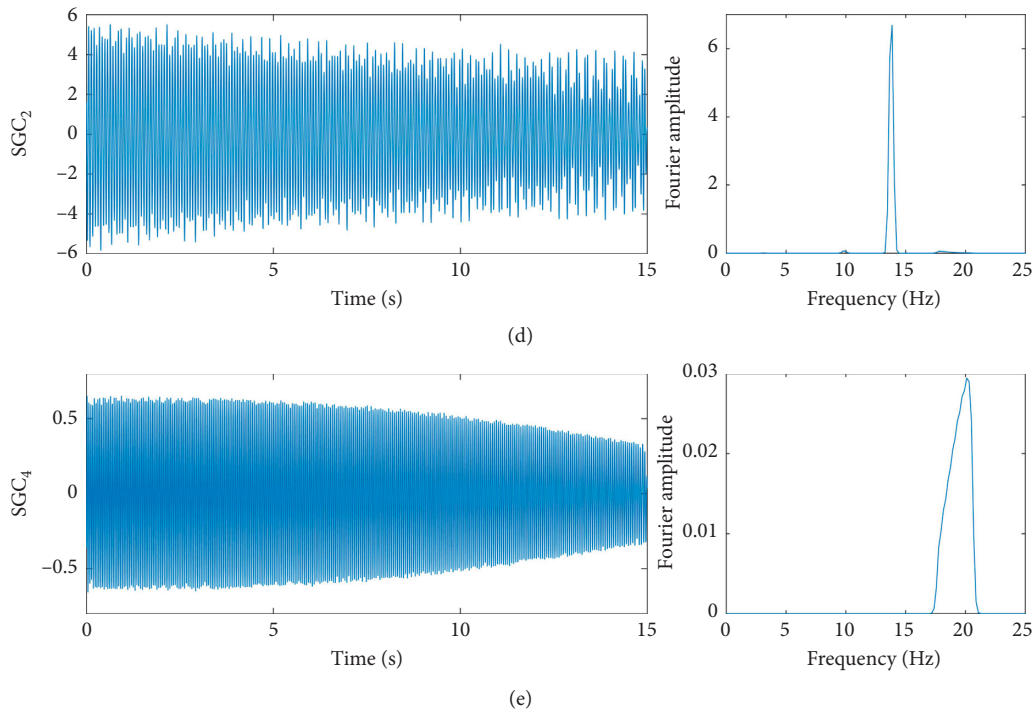

Figure 8: Decomposed symplectic geometric components (SGCs) of the response signal with symplectic geometric model decomposition in the simulation study (Case 2).

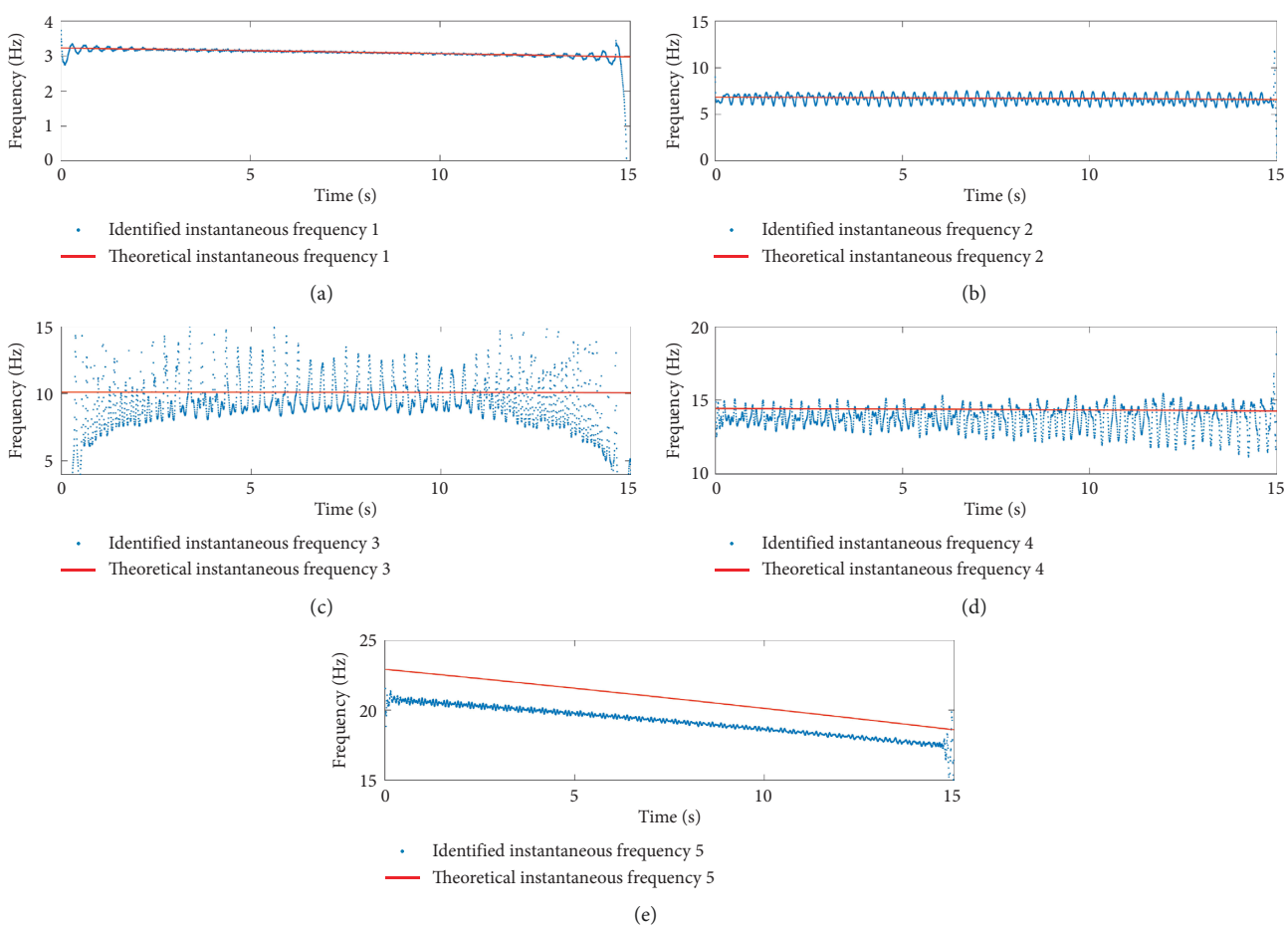

Figure 9: Symplectic geometric model decomposition applied to identify instantaneous frequencies in the simulation study (Case 2).

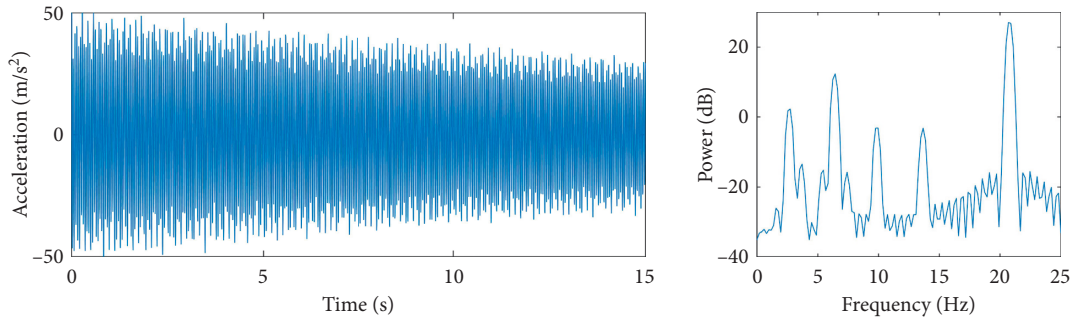

Figure 10: The results in the simulation study (Case 3): time-domain response signal as well as the fast Fourier transform spectrum.

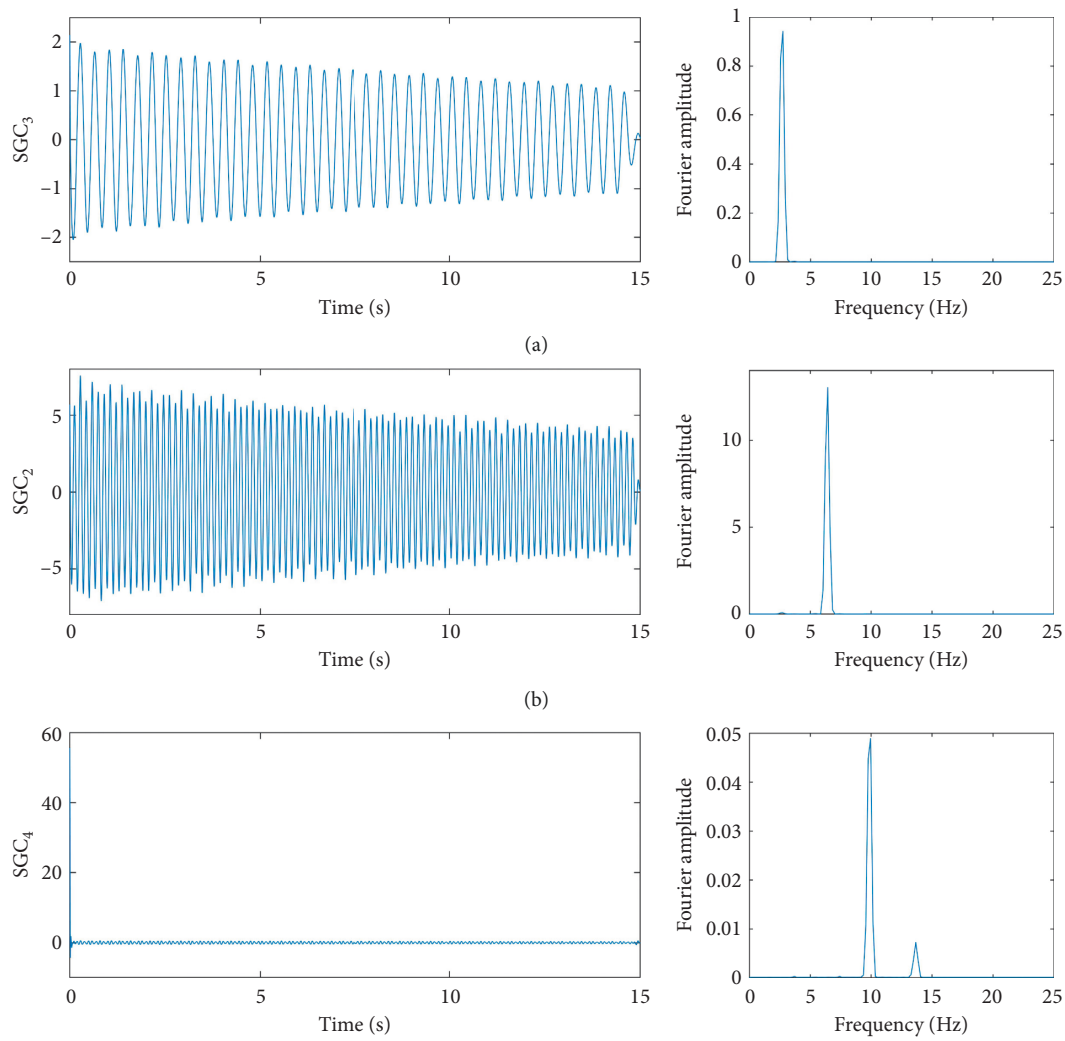

Figure 11: Continued.

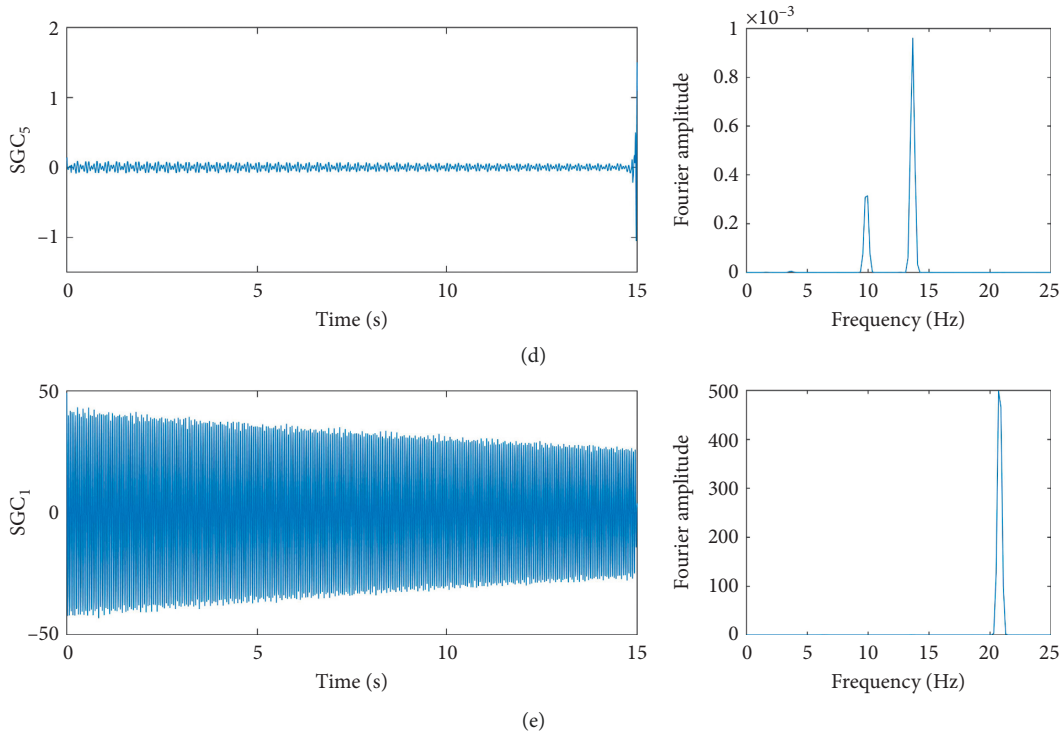

Figure 11: Decomposed symplectic geometric components (SGCs) of the response signal with symplectic geometric model decomposition in the simulation study (Case 3).

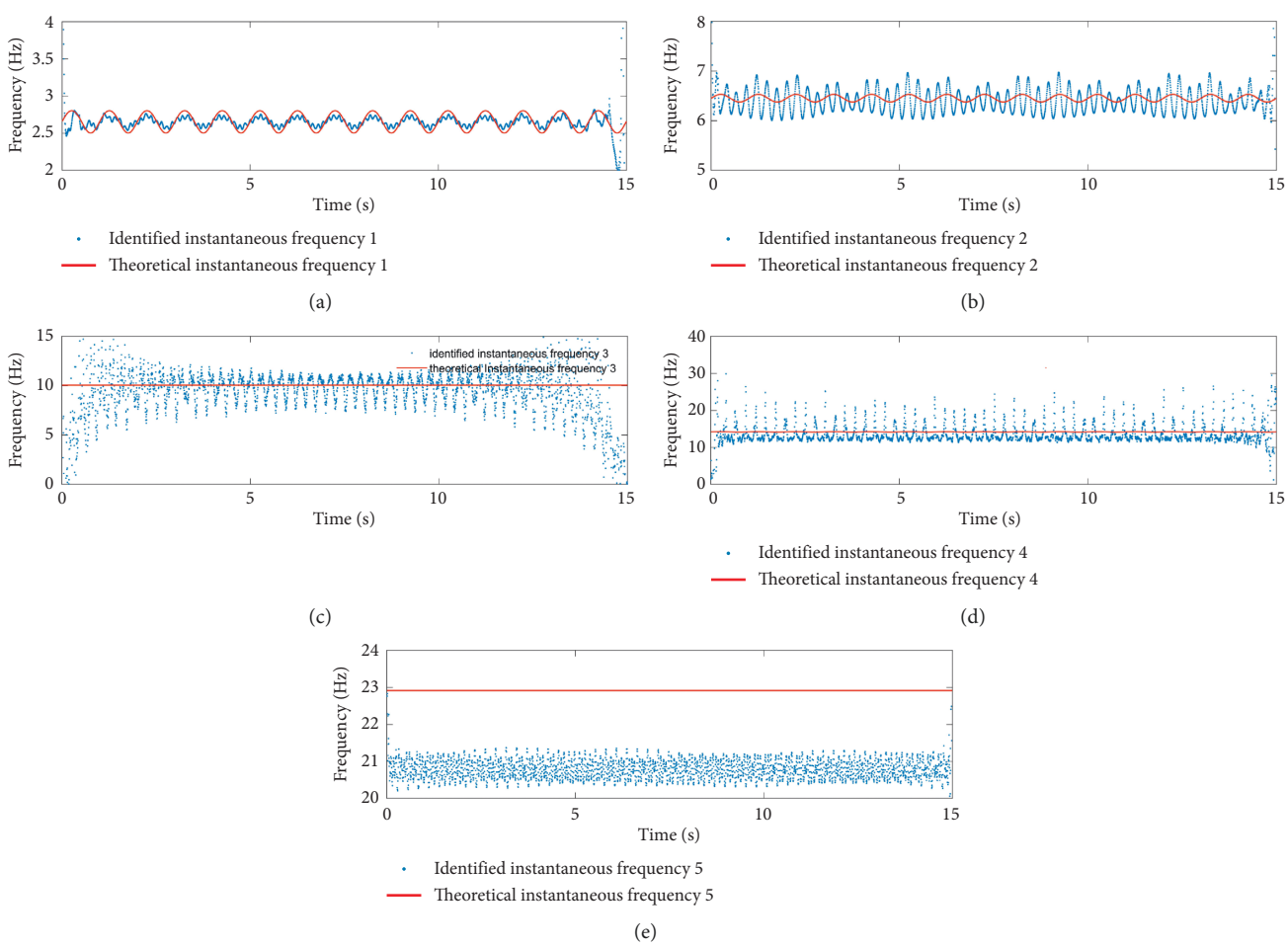

Figure 12: The results in the simulation study (Case 3): identified instantaneous frequencies by the symplectic geometric model decomposition.

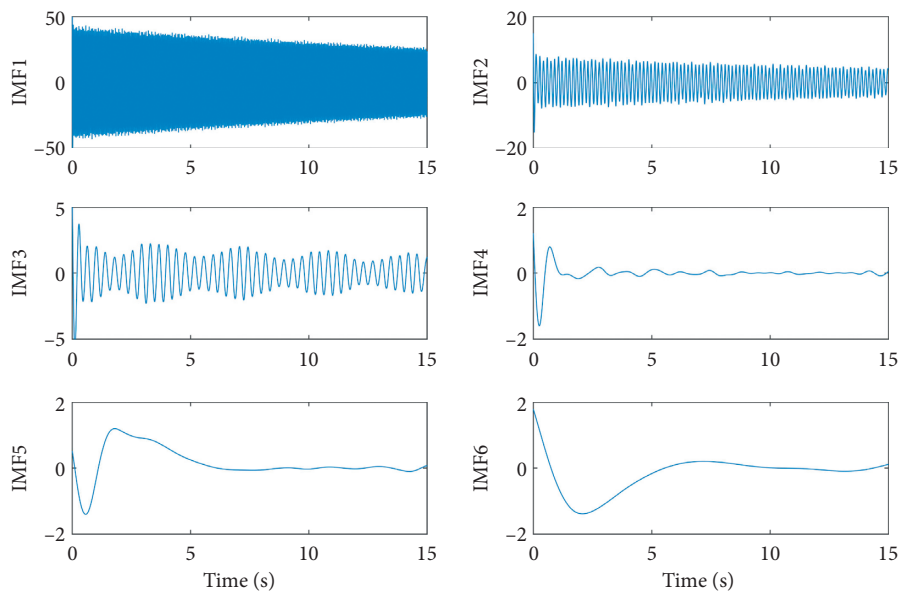

Figure 13: Extracted intrinsic model functions (IMFs) of the response signal on the basis of empirical model decomposition in the simulation study (Case 3).

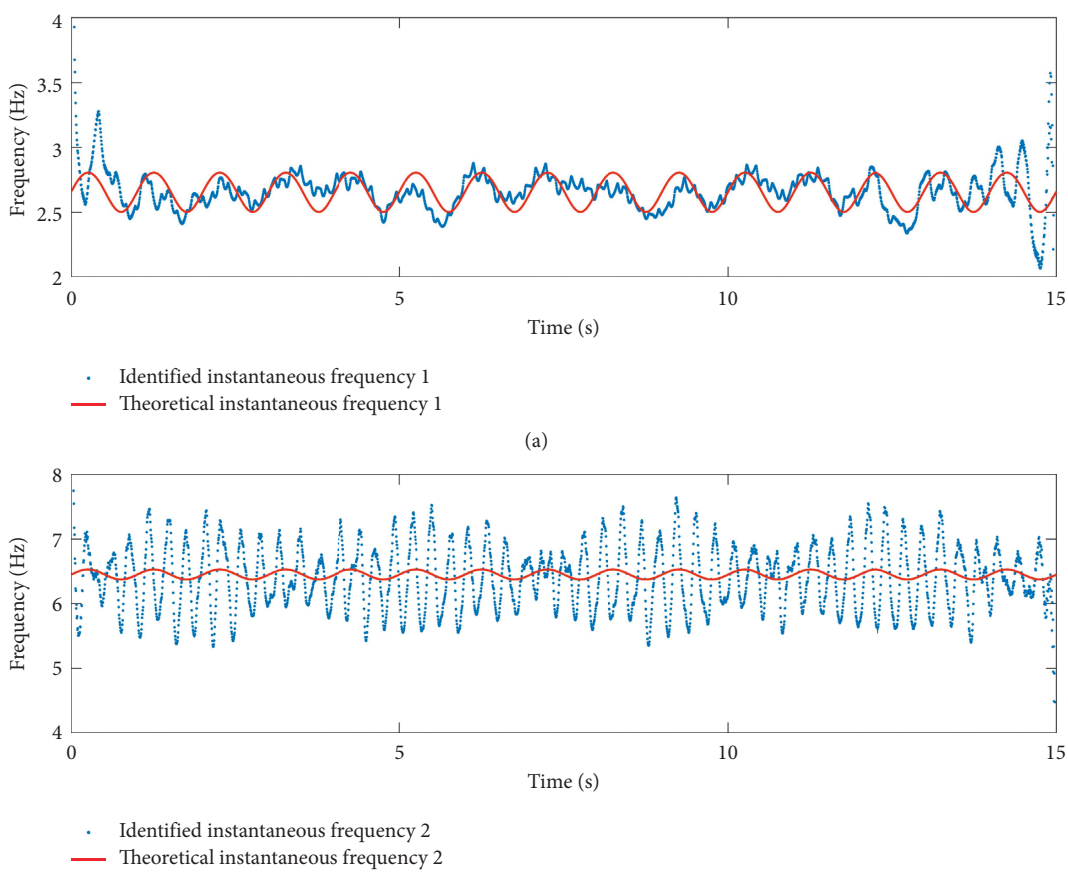

Figure 14: Continued.

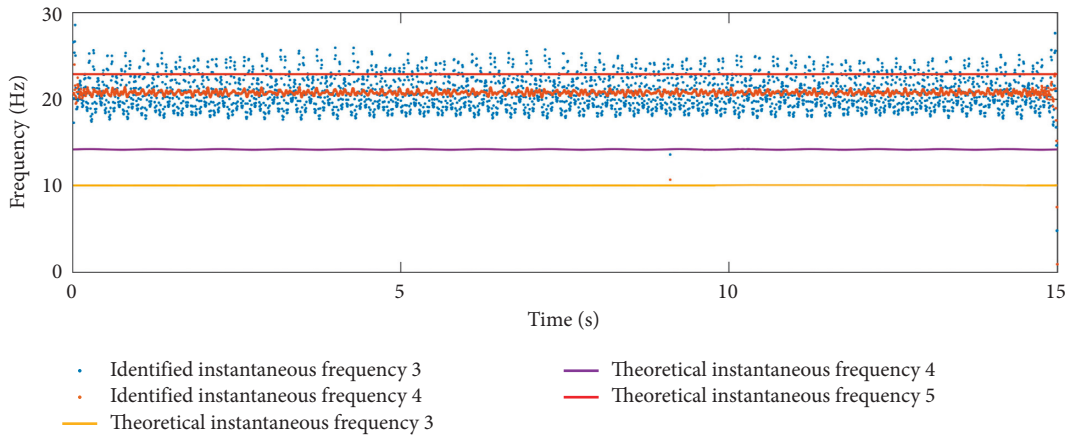

(c)

Figure 14: Identified instantaneous frequencies on the basis of empirical model decomposition in the simulation study (Case 3). (a) Identified instantaneous frequency from IMF 5. (b) Identified instantaneous frequency from IMF 4. (c) Identified instantaneous frequency from IMF 1–3.

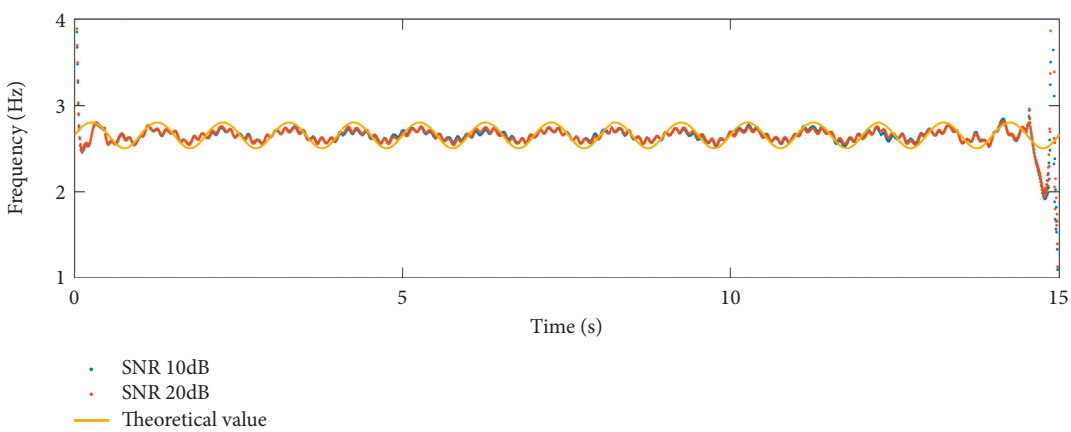

(a)

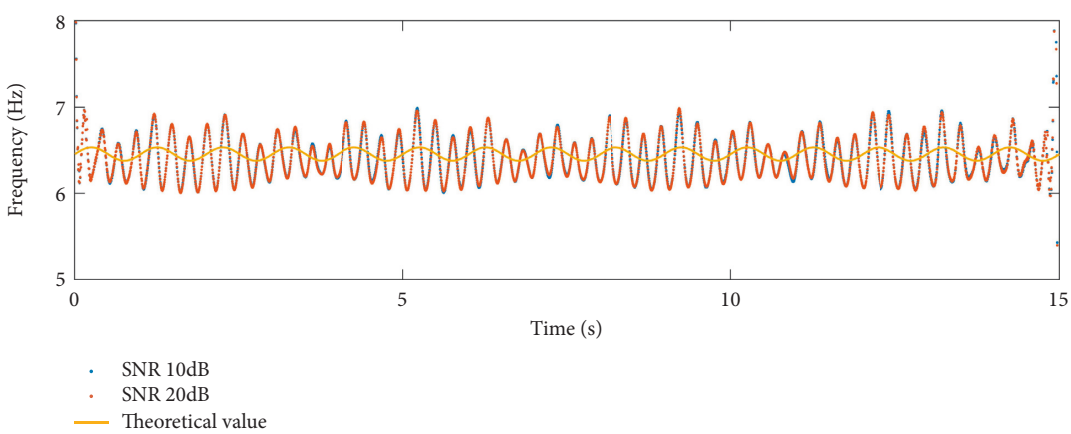

(b)

Figure 15: Continued.

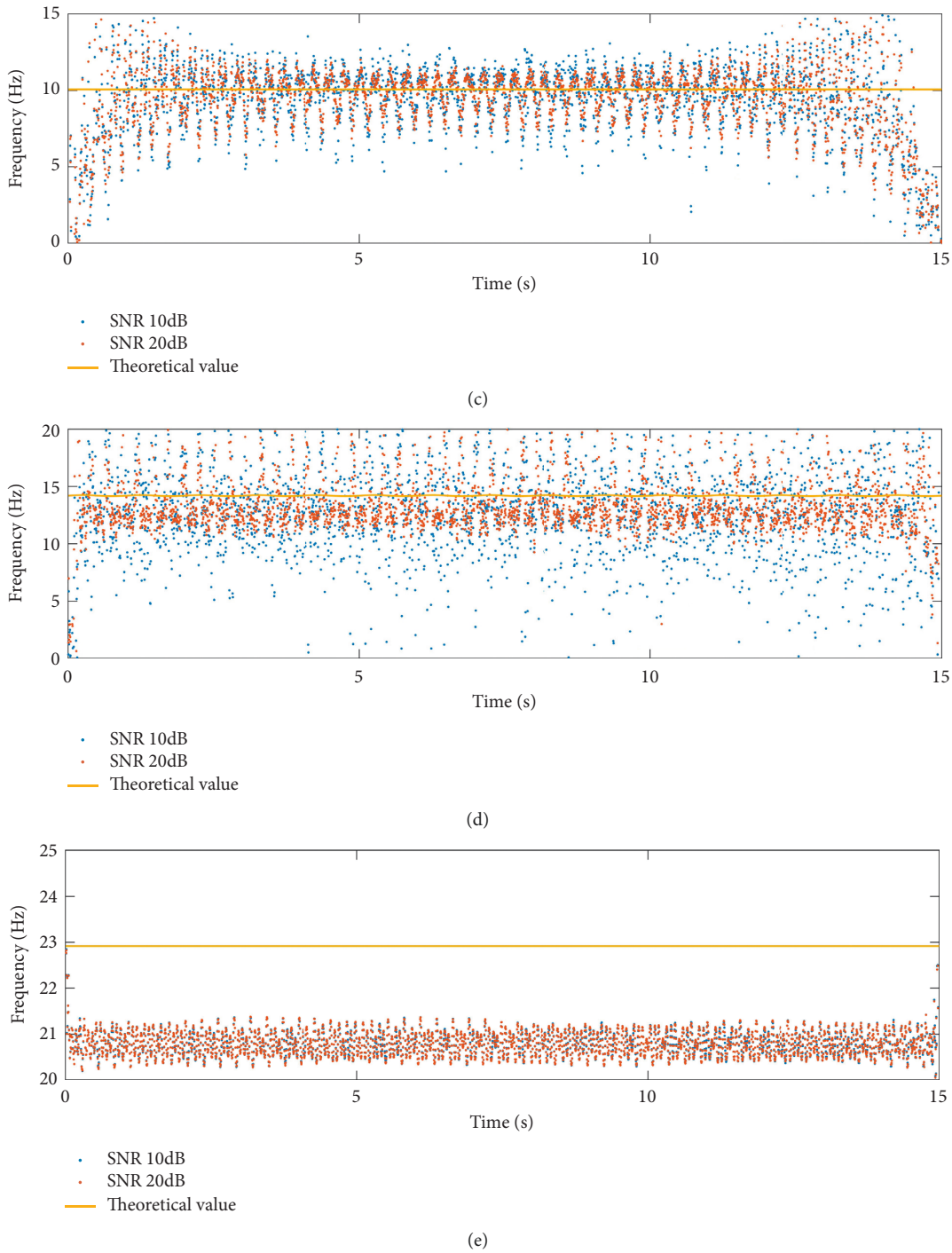

Figure 15: Identified instantaneous frequencies under different noise levels with symplectic geometric model decomposition in the simulation study (Case 3). (a) Identified instantaneous frequency of Mode 1. (b) Identified instantaneous frequency of Mode 2. (c) Identified instantaneous frequency of Mode 3. (d) Identified instantaneous frequency of Mode 4. (e) Identified instantaneous frequency of Mode 5.

proposed method to implement a better result. The second example is a time-variant structure, a wheel and rail vehicle system. Moreover, the signals measured from a moving vehicle are nonstationary. Those experiments can be implemented to prove the applicability and efficiency of instantaneous frequency identification and signal decomposition via SGMD.

4.1. Modal Identification of a Time-Invariant Structure. The applicability of the method proposed in this paper is demonstrated by the first example given in this section. A dissected vehicle under-frame crossbeam of high-speed train has been selected as the test object; usually the CRH3 high-speed train car body with 20 toes in crossbeams can improve the stiffness of car body and inhibit the chassis vertical

deformation. By adjusting the chassis beam, the natural frequency resonance of bodywork and bogie can be effectively avoided. To verify the accuracy of recognition results of experimental modal parameters, the finite element software Hypermesh and Nastran were used to complete the model grid division and modal calculation of the bottom crossbeams in this section. The material property was as follows: elastic modulus $E = 70\,\text{GPa}$, density of rho = $2710\,\text{kg/m}^3$, and Poisson's ratio $\mu = 0.33$.

This paper mainly analyzes the modal parameters of the crossbeam below 500 Hz, and the simulation results are shown in Figure 16. Considering the actual testing samples had two constraints, the vertical constraints are applied at the same position on geometry modal. The results of finite element analysis indicate that the first three models of vibration are larger in each sequence at the upper corner of the crossbeam, and the transverse response is larger than the vertical response because of the applied constraints. Therefore, as shown in Figure 17, an acceleration sensor is placed above the crossbeam to obtain vertical and horizontal vibration signals during the experiment. The testing material was made of aluminum alloy, but the sensor mass was closed to 1% of the beam mass. Therefore, to decrease the mass effect from the sensor in measurement, only one acceleration sensor was placed. The crossbeam was divided into 68 tapping points, and five times excitation induced by a hammer were applied on each tapping point. This hammer was connected to the 24 bit NI USB-6255DAQ board via a charge amplifier. The accelerometer is directly connected to the NI USB-6255 for signal acquisition. The acquisition duration is 5 s per test, and the sampling frequency is 10 kHz.

Before applying the method of this paper, the test results firstly need to be carried into preprocess for better identification of modal parameters. The acoustic and vibration output signals are as shown in Figure 18(a), and the Fourier transform is performed on the input hammer signal and the output signal; also, the ratio of self power spectrum to the cross power spectrum is obtained to get the estimated frequency response function of $H1$. These results are shown in Figure 18(b). Then, the means of 5 times $H1$ for each measurement point have been calculated and then inverse fast Fourier transform was performed; the time-domain response curve obtained by the preprocessing is subjected to modal parameter identification according to the symplectic geometric model decomposition method described above, and it is shown in Figure 18(c).

The method proposed in the Section 2.4 is used to identify the time-domain response signal of bottom crossbeam. The modal parameters of right singular value matrix after decomposition are shown in Table 2. Since the laboratory test is conducted by means of SISO multiple measurements, the cumulative error of the vibration model of the measuring point is large, and the result of vibration model is not ideal. Therefore, it would not be shown here. There is a large difference between the experimental and simulation results, and this error is caused by the damping here, which is not added in the simulation model.

The vibration of structure causes a change in the sound pressure of the surrounding medium. For a vibrating plate structure in the sound field, the plate can be divided into a limited number of small units. Those small units which are closely positioned on the surface of the plate can be assumed as point sources in the sound pressure measurement. Therefore, where the distances are relatively close, the sound pressure of the measuring point is proportional to the vibration acceleration of the reference point. Prezelj et al. [31] have also verified the relationship between the near-field sound pressure generated by the vibrational radiation of flat structure and dynamic response of the structure.

In addition, Table 3 shows that the first- and third-order modal recognition results are closer to the simulation results than those of the vibration recognition. However, the second-order errors are larger. According to those results, the method is applicable to the identification of structural modal parameters of near-field sound pressure signals. It should be noted that when applying the sound pressure signal to identify the structural modal parameters, the distance between the microphone and the structure should be as small as possible so that effectiveness of the air damping can be ignored during the sound wave propagation process.

Both simulation and experimental results confirm that the method proposed in this paper can be used to achieve the accuracy and consistency of modal parameters. However, in the data processing, since each layer of SGC is extracted, it is necessary to repeat the construction matrix. Therefore, a large number of repeated calculations are required. Actually, this method is a time-domain decomposition method and it is very sensitive to the data length, as shown in the time-domain diagram in Figures 19 and 20, when the time-domain response signal is decomposed. However, the test of output signal length is 5 s. If the data length of the decomposed SGC signal is greater than 1 s, the vibration signal has been attenuated to a very small value, and the modal identification will contribute to increase the identify accuracy under the appropriate adjustment of data length after decomposition. However, in this paper, there are much more points in the experimental model, and all response time is unified to 2.5 s.

4.2. Instantaneous Frequency Identification of a Time-Variant System. The second example is shown in Figure 21, which is a time-variant wheel-rail coupling system. A field braking test was carried out here on the tangent ballast track. The test line's length was close to 1500 m. The test train comprised three HX-type heavy haul locomotives which are widely employed in 10,000 t freight trains connected by 100-type coupler and draft gear systems. It was reported that a bogie frame had a natural frequency similar to the excitation frequencies which were included in the time-variant loads and that this similarity resulted in fatigue damage in the bogie frame [32]. If the track clearance on the track is large, the natural frequency of the bogie will be frequently excited, and thus detecting the excitation frequency of bogie frame and time-variant load has vital engineering values. According to the literature [33], any interaction between external excitations and natural vibration models is primarily located at relatively low-frequency regime below 200 Hz. Four acceleration sensors are placed above the bogie frame to record the

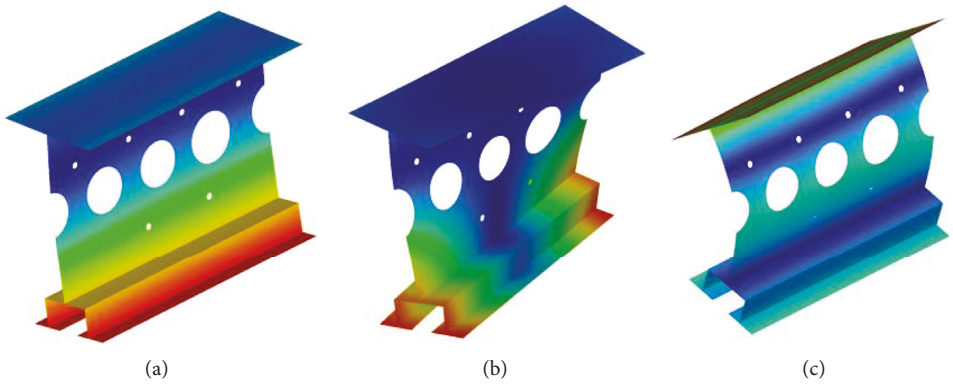

Figure 16: The first three models of simulation. (a) Mode Frequency = 65.0 Hz. (b) Mode Frequency = 214.1 Hz. (c) Mode Frequency = 447.1 Hz.

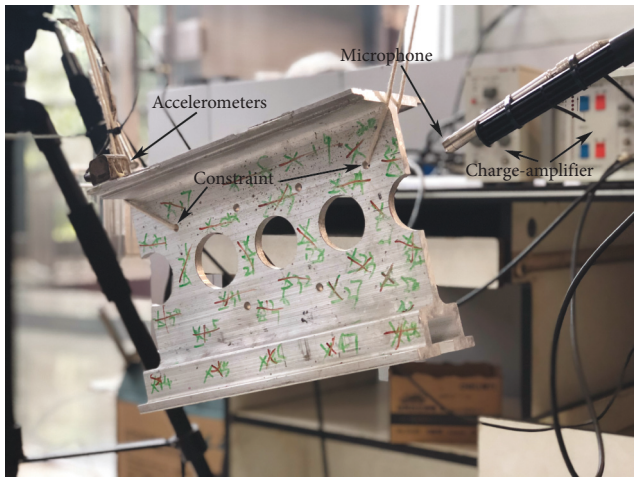

Figure 17: Experimental setup.

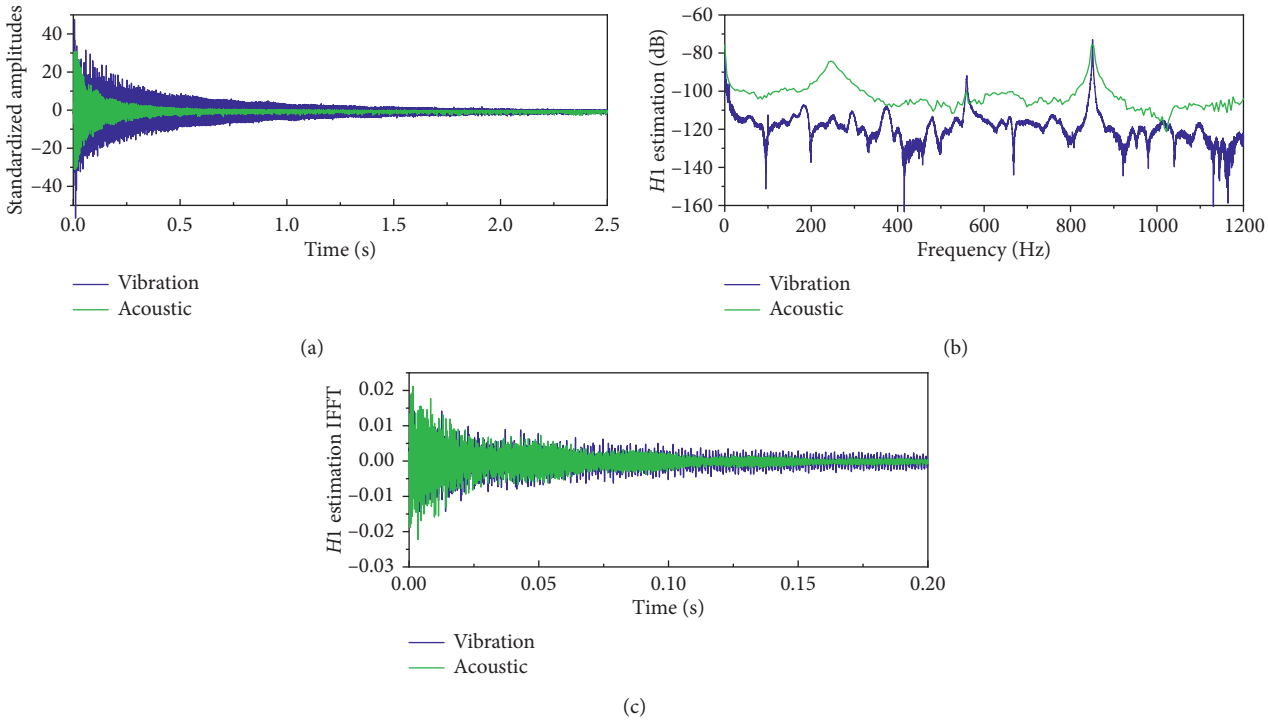

Figure 18: The acoustic and vibration signals. (a) Time series of acoustic and vibration signals. (b) $H1$ estimation frequency response functions. (c) $H1$ estimation inverse fast Fourier transform.

Table 2: The modal identification of vibration signals.

	Natural frequency	Error (%)	Damping ratio
Model 1	62.92	3.2	0.00213
Model 2	215.82	0.80	0.00073
Model 3	397.11	11.18	0.00029

Table 3: The results of acoustic identification.

	Natural frequency	Error (%)	Damping ratio
Model 1	69.0	6.15	0.0012
Model 2	246.3	15.04	0.0010
Model 3	425.3	4.88	0.0005

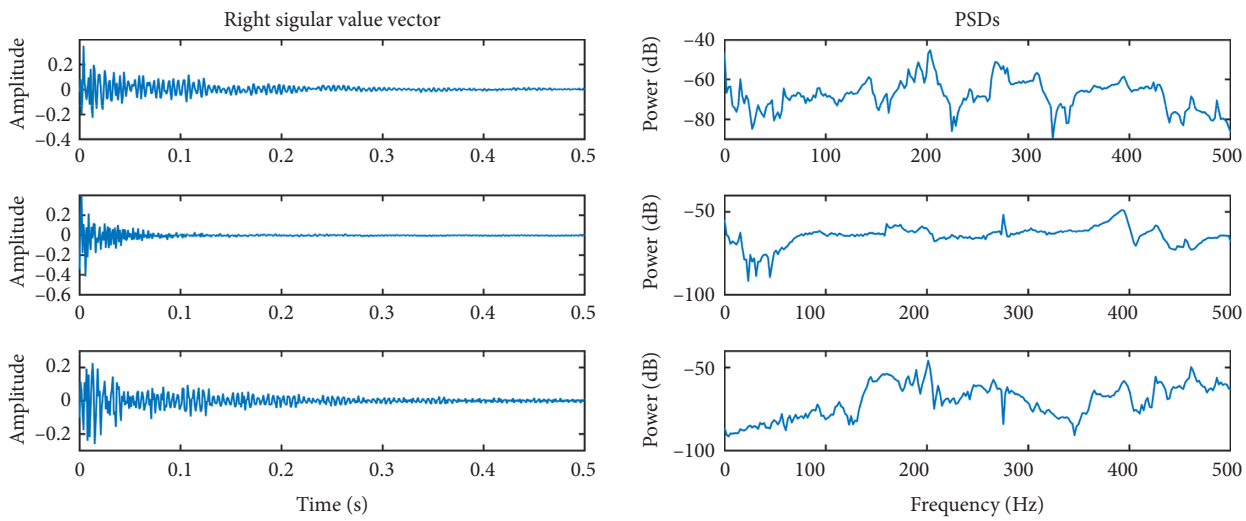

Figure 19: The first three models of vibration signal identification results.

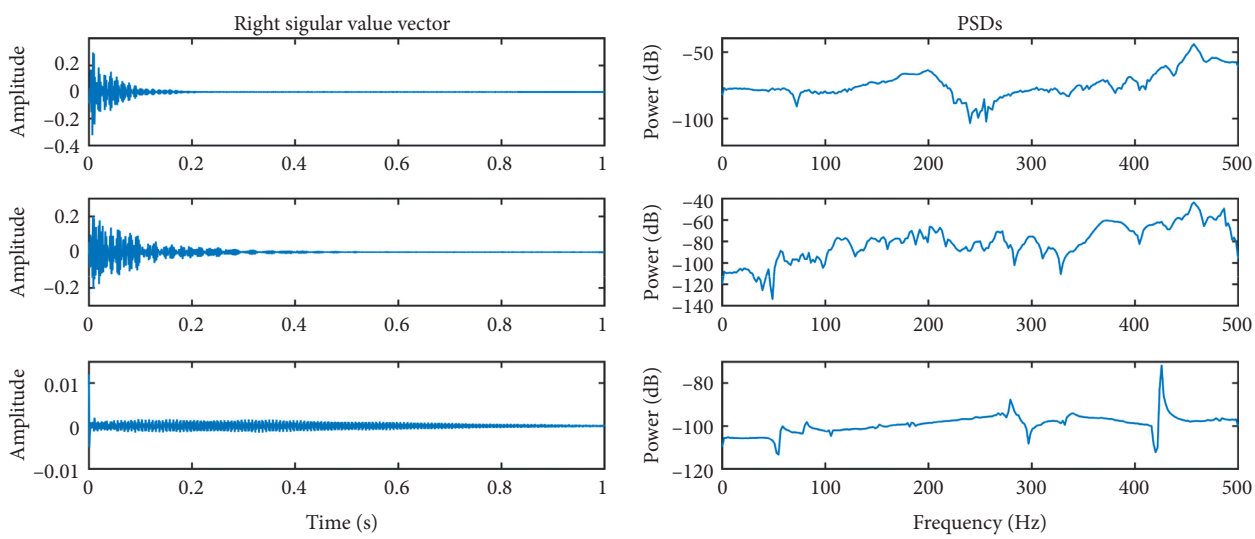

Figure 20: The first three models of acoustic signals identification results.

dynamic response of the moving vehicle. When the vehicle speed reached 80 km/h, resistance braking was performed and response data of about 9 seconds were recorded. The band-pass range is set to 0–100 Hz, with a sampling frequency of 5000 Hz. The time history of the acceleration response on the bogie during braking of the vehicle and its Fourier spectrum are shown in Figure 22. Moreover, we can see that the energy is primarily within a scope of 2–80 Hz. Approximately 63 Hz

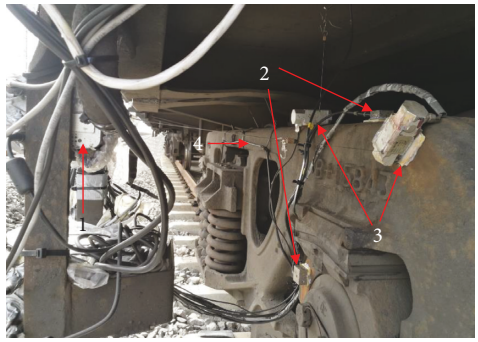

Figure 21: Test device for wheel and rail system in field test. 1: signal acquisition device; 2: acceleration sensor; 3: displacement sensor; 4: bogie.

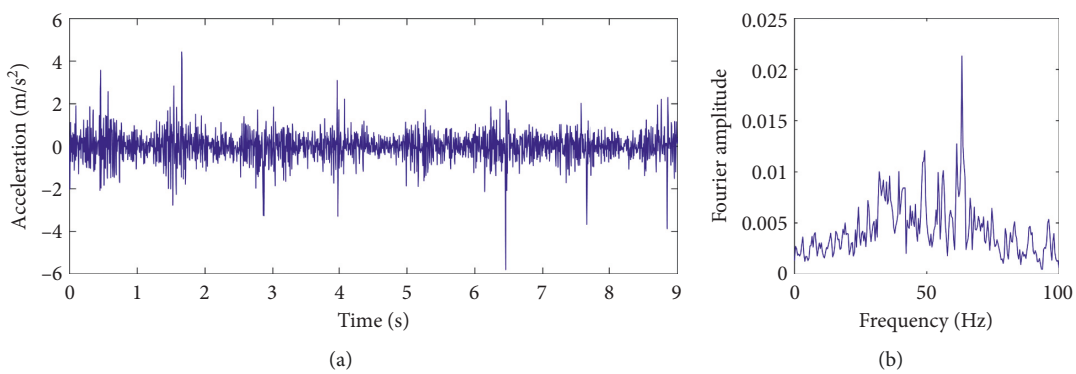

Figure 22: Wheel-rail coupling system: time history and fast Fourier transform spectrum of measured response.

corresponds to the maximum energy, and the frequency range from 30 to 70 Hz corresponds to the significant vibrations. It is obvious from the time history that there is a significant time-variant load excitation when the vehicle passes near the rail joint gap. If the moving vehicle locations are changed, the vibration characteristics of the system are also changed. During the running process of the vehicle, there are significant fluctuations and noise in the response signal.

Hence, the method proposed and the conventional EMD method, as well as the measured acceleration response, were used for the identification of the instantaneous frequency of time-variant systems. Figures 23 and 24 show the identified results from these two methods, respectively. The EMD method has a large number of ripple phenomena and overlaps at the instantaneous frequency, and there is no significant continuous frequency near the main frequency of 63 Hz in the Fourier spectrum. Meanwhile, the SGMD method described in this paper can effectively suppress the ripple phenomenon and overlap. Based on the results of past studies [33–35], the response reason for each SGC is determined. Also, the SGMD decomposes the acceleration response signal into 10 SGCs components. As shown in Figure 24, SGC_2 is the second-order natural frequency of the frame and external excitation (80 Hz–100 Hz); SGC_3 causes the bounce of the bogie frame (6–8 Hz); SGC_4 and SGC_7 are the wheel noncircular excitation (13.67 Hz, 27.73 Hz); SGC_5 and SGC_6 correspond to 0.39 Hz and 1.56 Hz, which are related to the low-frequency body and bogie rigid motion; SGC_8 is the rail surface excitation (3.12 Hz); SGC_9 450 is the first-order natural frequency of bogie frame (63.28 Hz). Among them, the first-order natural frequency of the bogie frame has obvious endpoint problems. SGC_1 and SGC_{10} instantaneous frequency distribution is in the entire analysis frequency band, so it is considered as noise and is not shown. Obvious fluctuations are observed within the identified instantaneous frequencies, which are caused by the uncertainties of wheel-rail coupling and measurement noise. Therefore, the efficiency and effectiveness of this method have been verified on identifying the instantaneous frequency of time-variant systems which have measurement noise as well as significant uncertainties.

5. Conclusions

The iterative method is introduced in the decomposition process of the symplectic geometry model decomposition, replacing the traditional similarity direct combination. Compared with other decomposition methods, SGMD does not need user-defined parameters and has better robustness and suppresses modal aliasing. The results show that better decomposition performance and robustness can be obtained by the proposed SGMD method, without setting user-defined parameters.

Moreover, a new modal parameter identification method is proposed for modal parameter identification using

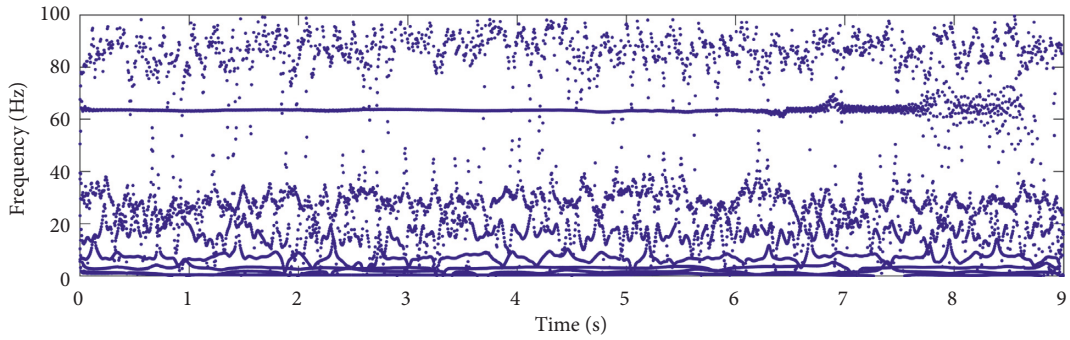

Figure 23: Identified instantaneous frequencies of wheel-rail coupling systems on the basis of empirical model decomposition.

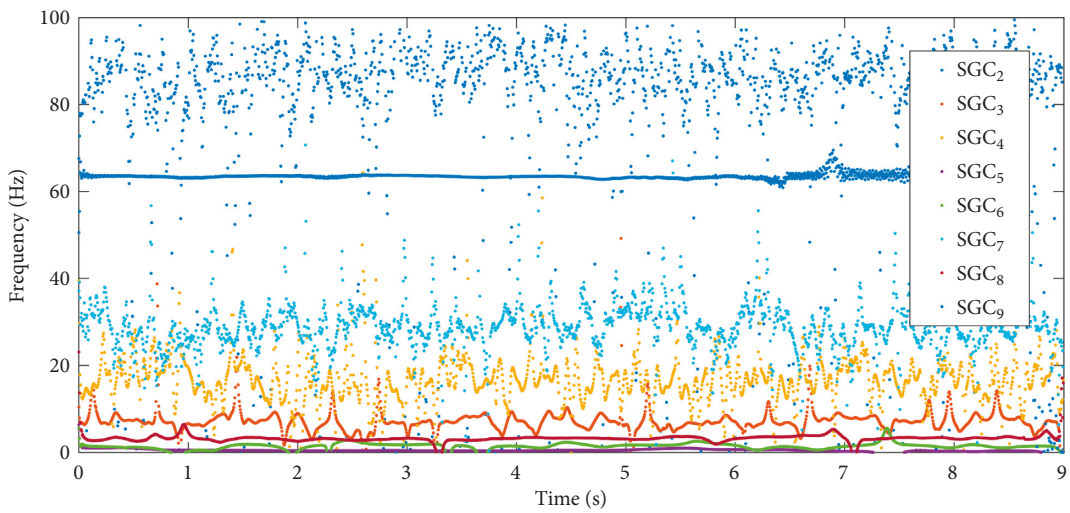

Figure 24: Identified instantaneous frequencies of wheel-rail coupling systems on the basis of symplectic geometry model decomposition.

symplectic geometry model decomposition. The core of this method is to solve the eigenvalues of Hamiltonian matrix by using symplectic geometric similarity transformation, and at the same time, the essential characteristics of the original signal can still be unchanged. It is proposed to calculate the normalized mean absolute errors which are between residual signals and original signals as the termination condition of decomposition. For the time-invariant structural model parameters, SVD is applied to decouple the modal, realize the identification of modal shape, and improve the recognition accuracy of the natural frequency and damping ratio directly via SGMD. Also, it is suitable to identify instantaneous frequencies of time-variant structures. The real response signal is decomposed into several SGCs, after which the Hilbert transform is utilized to recognize instantaneous frequency. Considering the three models of stiffness variation, simulation studies are carried out on time-invariant systems and time-variant systems to study the ability of the proposed method. Test and verification have been applied on the time-variant vehicle-rail beam and test line wheel-rail coupling system in the laboratory; also, the proposed method should been confirmed for applying the analysis of time-frequency and the instantaneous frequency identification of time-variant systems with nonstationary variable signal.

The experiments using simulated and real data show that the proposed method can make good use of the limited bandwidth of each model for signal decomposition, and it can also accurately extract the instantaneous frequency of the time-variant system. This method can be applied to signal decomposition as well as the modal identification of structures under environment excitation, whereas, it is not the key problem in this article. Further research will be performed to study the applicability of modal identification time-invariant and variant structures under environment excitation. In addition, compared with the same signal-based adaptive method (such as EMD), the SGMD-based system identification method has better robustness to noise and sampling frequency. There are still many problems in modal parameter identification for symplectic geometry decomposition, such as how to further improve the MAC of the mode, speeding up the calculation of SGMD, and solving reconstruction constraints and their end effects. Hence, in future research, the authors will pay more attention to these issues.

Data Availability

The data used to support the findings of this study have been deposited in the FIGSHARE repository (https://doi.org/10.6084/m9.figshare.7610429.v1).

Conflicts of Interest

The authors declare that they have no conflicts of interest.

Acknowledgments

This paper was supported by the National Key Research and Development Program of China (2016YFB1200401-102 and 2018YFB1201605) and the Sichuan Science and Technology Program (2019YFG0102).

References

[1] Z.-H. Min, L.-M. Sun, Z. Sun, and D.-H. Dan, "Modal parameter identification method based on wavelet transform and singular value decomposition," *Journal of Tongji University (Natural Science)*, vol. 37, pp. 460–465, 2009.

[2] X. Sun, M. Hao, and L. Zhang, "Research on broadband modal parameters identification under ambient excitation," *Journal of Building Structures*, vol. 32, pp. 151–156, 2011.

[3] B. H. Kim, N. Stubbs, and T. Park, "A new method to extract modal parameters using output-only responses," *Journal of Sound and Vibration*, vol. 282, no. 1-2, pp. 215–230, 2005.

[4] R. Brincker, L. Zhang, and P. Andersen, "Modal identification of output-only systems using frequency domain decomposition," *Smart Materials and Structures*, vol. 10, no. 3, pp. 441–445, 2001.

[5] L. Faravelli, F. Ubertini, and C. Fuggini, "System identification of a super high-rise building via a stochastic subspace approach," *Smart Structures and Systems*, vol. 7, no. 2, pp. 133–152, 2011.

[6] J.-N. Juang and R. S. Pappa, "An eigensystem realization algorithm for modal parameter identification and model reduction," *Journal of Guidance, Control, and Dynamics*, vol. 8, no. 5, pp. 620–627, 1985.

[7] Q. Qin, H. B. Li, L. Z. Qian, and C.-K. Lau, "Modal identification of Tsing Ma bridge by using improved eigensystem realization algorithm," *Journal of Sound and Vibration*, vol. 247, no. 2, pp. 325–341, 2001.

[8] J. M. Caicedo, S. J. Dyke, and E. A. Johnson, "Natural excitation technique and eigensystem realization algorithm for phase I of the IASC-ASCE benchmark problem: simulated data," *Journal of Engineering Mechanics*, vol. 130, no. 1, pp. 49–60, 2004.

[9] M. Doehler, X.-B. Lam, and L. Mevel, "Uncertainty quantification for modal parameters from stochastic subspace identification on multi-setup measurements," *Mechanical Systems and Signal Processing*, vol. 36, no. 2, pp. 562–581, 2013.

[10] F.-L. Zhang, Y.-C. Ni, S.-K. Au, and H.-F. Lam, "Fast Bayesian approach for modal identification using free vibration data, part I—most probable value," *Mechanical Systems and Signal Processing*, vol. 70-71, pp. 209–220, 2016.

[11] W.-J. Yan and L. S. Katafygiotis, "A novel Bayesian approach for structural model updating utilizing statistical modal information from multiple setups," *Structural Safety*, vol. 52, pp. 260–271, 2015.

[12] S. Sankararaman and S. Mahadevan, "Bayesian methodology for diagnosis uncertainty quantification and health monitoring," *Structural Control and Health Monitoring*, vol. 20, no. 1, pp. 88–106, 2013.

[13] K.-V. Yuen and J. L. Beck, "Updating properties of nonlinear dynamical systems with uncertain input," *Journal of Engineering Mechanics*, vol. 129, no. 1, pp. 9–20, 2003.

[14] G. Li and Q. Weilian, "Damage detection of bars based on strain mode and bayesian statistical method," *Journal of Wuhan University of Technology*, vol. 29, pp. 135–138, 2007.

[15] H. Pan and Z. Xie, "Modified bayesian spectral density approach and its application to modal parameter identification of super-tall building," *Journal of Building Structures*, vol. 37, no. 12, pp. 27–32, 2016.

[16] J. Hu, H.-F. Lam, and J.-H. Yang, "Operational modal identification and finite element model updating of a coupled building following Bayesian approach," *Structural Control & Health Monitoring*, vol. 25, no. 2, 2018.

[17] J. P. Noël and G. Kerschen, "Nonlinear system identification in structural dynamics: 10 more years of progress," *Mechanical Systems and Signal Processing*, vol. 83, pp. 2–35, 2017.

[18] D. J. Ewins, B. Weekes, and A. Delli Carri, "Modal testing for model validation of structures with discrete nonlinearities," *Philosophical Transactions of the Royal Society A: Mathematical, Physical and Engineering Sciences*, vol. 373, no. 2051, article 20140410, 2015.

[19] L. Faravelli, C. Fuggini, and F. Ubertini, "Toward a hybrid control solution for cable dynamics: theoretical prediction and experimental validation," *Structural Control & Health Monitoring*, vol. 17, no. 4, pp. 386–403, 2010.

[20] L. Xu and X. Chen, "Random analysis on vibration sources of train-track system," *Journal of the China Railway Society*, vol. 39, pp. 9–16, 2017.

[21] Y. Yang, Z. Peng, W. Zhang, and G. Meng, "Parameterised time-frequency analysis methods and their engineering applications: a review of recent advances," *Mechanical Systems and Signal Processing*, vol. 119, pp. 182–221, 2019.

[22] M. Mihalec, J. Slavič, and M. Boltežar, "Synchrosqueezed wavelet transform for damping identification," *Mechanical Systems and Signal Processing*, vol. 80, pp. 324–334, 2016.

[23] L. A. Montejo and A. L. Vidot-Vega, "Synchrosqueezed wavelet transform for frequency and damping identification from noisy signals," *Smart Structures and Systems*, vol. 9, no. 5, pp. 441–459, 2012.

[24] H. Li, X. Deng, and H. Dai, "Structural damage detection using the combination method of EMD and wavelet analysis," *Mechanical Systems and Signal Processing*, vol. 21, no. 1, pp. 298–306, 2007.

[25] Z. Y. Shi and S. S. Law, "Identification of linear time-varying dynamical systems using Hilbert transform and empirical mode decomposition method," *Journal of Applied Mechanics*, vol. 74, no. 2, pp. 223–230, 2007.

[26] P. Ni, J. Li, H. Hao et al., "Time-varying system identification using variational mode decomposition," *Structural Control & Health Monitoring*, vol. 25, no. 6, article e2175, 2018.

[27] H. Xie, Z. Wang, and H. Huang, "Identification determinism in time series based on symplectic geometry spectra," *Physics Letters A*, vol. 342, no. 1-2, pp. 156–161, 2005.

[28] H. Pan, Y. Yang, X. Li, J. Zheng, and J. Cheng, "Symplectic geometry mode decomposition and its application to rotating machinery compound fault diagnosis," *Mechanical Systems and Signal Processing*, vol. 114, pp. 189–211, 2019.

[29] P. Bonizzi, J. M. H. Karel, O. Meste, and R. L. M. Peeters, "Singular spectrum decomposition: a new method for time series decomposition," *Advances in Adaptive Data Analysis*, vol. 6, no. 4, article 1450011, pp. 107–109, 2015.

[30] J. E. Cooper, "Identification of time varying modal parameters," *The Aeronautical Journal*, vol. 94, no. 938, pp. 271–278, 1990.

[31] J. Prezelj, P. Lipar, A. Belšak, and M. Č.lšak, "On acoustic very near field measurements," *Mechanical Systems and Signal Processing*, vol. 40, no. 1, pp. 194–207, 2013.
[32] J. T. Pearson, R. M. Goodall, T. X. Mei, and G. Himmelstein, "Active stability control strategies for a high speed bogie," *Control Engineering Practice*, vol. 12, no. 11, pp. 1381–1391, 2004.
[33] Y. Lu, P. Xiang, P. Dong, X. Zhang, and J. Zeng, "Analysis of the effects of vibration modes on fatigue damage in high-speed train bogie frames," *Engineering Failure Analysis*, vol. 89, pp. 222–241, 2018.
[34] H. Shi, J. Wang, P. Wu, C. Song, and W. Teng, "Field measurements of the evolution of wheel wear and vehicle dynamics for high-speed trains," *Vehicle System Dynamics*, vol. 56, no. 8, pp. 1187–1206, 2018.
[35] J. Liu, Y. Zhao, L. Ling, and X.-Z. Sheng, "Operational modal analysis of bogie frame and its effect on vibration transfer of high-speed train," *Noise and Vibration Control*, vol. 35, no. 3, pp. 19–23, 2015.